Timeline on the application of intercalation materials in Capacitive Deionization

K. Singh[a,b], S. Porada[b,c], H.D. de Gier[b], P.M. Biesheuvel[b], L.C.P.M. de Smet[a,b,*]

[a] Laboratory of Organic Chemistry, Wageningen University & Research, Stippeneng 4, 6708 WE Wageningen, The Netherlands
[b] Wetsus, European Centre of Excellence for Sustainable Water Technology, Oostergoweg 9, 8911 MA Leeuwarden, The Netherlands
[c] Soft Matter, Fluidics and Interfaces Group, Faculty of Science and Technology, University of Twente, Drienerlolaan 5, 7522 NB Enschede, The Netherlands

A B S T R A C T

Capacitive deionization is a water desalination technology in which ions are stored in electrodes in an electrochemical cell construction, connected to an external circuit, to remove ions present in water from various sources. Conventionally, carbon has been the choice of material for the electrodes due to its low cost, low contact resistance and high specific surface area, electronic conductivity, and ion mobility within pores. The ions in the water are stored at the pore walls of these electrodes in an electrical double layer. However, alternative electrode materials, with a different mechanism for ion and charge storage, referred to as ion intercalation, have been fabricated and studied as well. The salt adsorption performance exhibited by these materials is in most cases higher than that of carbon electrodes. This work traces the evolution of the study of redox activity in these intercalation materials and provides a chronological description of major developments in the field of Capacitive Deionization (CDI) with intercalation electrodes. In addition, some insights into the cell architecture and operation parameters are provided and we present our outlook of future developments in the field of intercalation materials for CDI.

1. Introduction

The electrochemical technology of Capacitive Deionization (CDI) has witnessed an exponential increase in research and development efforts over the past years. It employs porous electrodes to remove ions of interest from water. These ions are driven to the interior of the electrodes by the electrical current, where they are stored. The mechanism of ion storage in CDI depends on the type of electrode material. The mechanism can be ion adsorption next to a charged interface, or ion insertion into a host lattice, which may or may not be followed by a change in the redox state of an element constituting the lattice. The first category consists of carbon-based electrodes which have been studied [1–4] and reviewed thoroughly [5–7]. Similar literature is available for non-carbon electrodes for applications in energy storage [8,9] and desalination [10–12]. However, no attempt has been made to record the use of intercalation materials in the rapidly growing field of CDI. The current work intends to fill this gap by providing a review in the form of a timeline overview on the use of inorganic ion intercalation materials as electrodes for water desalination by CDI. We also address selected papers from other fields (e.g., batteries) that inspired the use of such materials for water desalination.

Research into cheaper alternative, materials for Li-ion batteries led to research into aqueous sodium and potassium ion batteries, due to their low cost and easy availability [9]. As a consequence, transition metal compounds such as $NaMnO_2$ [13], $Na_2Fe_2P_2O_7$ [14], and Na_2Ni [Fe(CN)$_6$ (NiHCF) [15] were nominated as promising candidates for aqueous ion batteries. Since CDI requires storage of ions in the electrodes of a desalination cell, the electrode materials used for batteries satisfy this condition of being capable of ion storage as well.

Carbon as an electrode material has been in use in CDI since the 1960s [16,17]. However, intercalation materials have certain key advantages in comparison to carbon as electrodes in CDI. The first advantage is the ability of intercalation materials such as nickel hexacyanoferrate (NiHCF) to provide the same salt adsorption capacity (SAC) at a lower voltage. Therefore, these materials have a lower energy input than carbon electrodes. This is attributed to a higher differential charge, $\frac{\partial Q}{\partial E}$ where Q is the charge input/output and E is the corresponding change in the electrode potential, in comparison to carbon [18]. Differential charge values are reported to be an order of magnitude higher for NiHCF electrodes than those for carbon electrodes [18]. Therefore, the use of intercalation materials may potentially reduce energy consumption while keeping SAC unchanged. Secondly, carbon electrodes suffer from co-ion expulsion, a phenomenon where co-ions are depleted from the electrical double layer (EDL) during ion removal from the salt solution [19]. With carbon electrodes, it has been observed that an increase in the salinity of the water leads to a decrease in the salt adsorption, and consequently leads to a decrease in the charge efficiency (i.e. the moles of salt adsorbed/moles of charge input) [19,20]. This effect can be minimized by placing ion-selective membranes in between the electrodes and the salt solution as done in
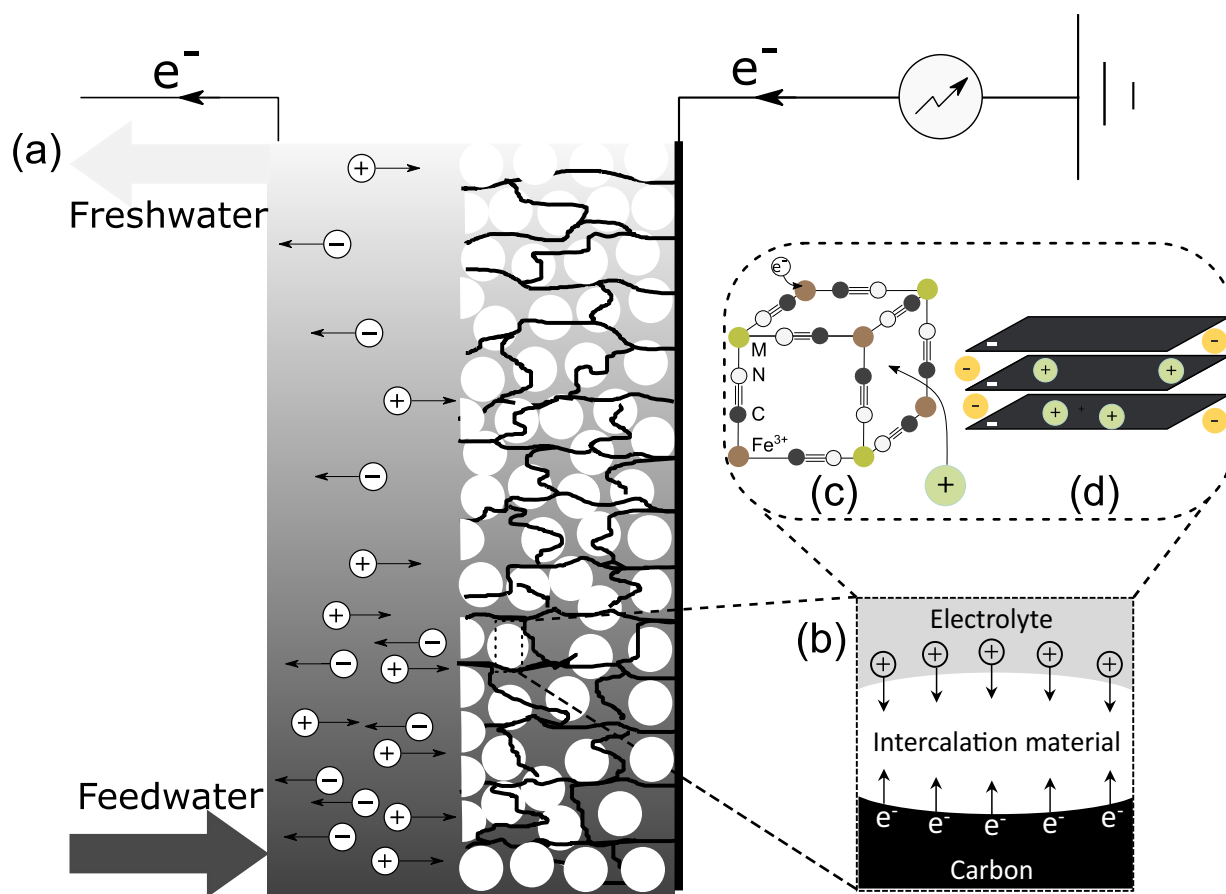
Fig. 1. (a) Schematic illustration of an intercalation material being used as an electrode in a CDI cell. Salt concentration in the flow channel adjacent to the electrode undergoing intercalation decreases with time, indicated by the grey-scale gradient. Black lines in the electrode area represent the conductive carbon which provides an electronic link between the intercalation particles (white circles) and the current collector. (b) Schematic representation of intercalation of cations and inclusion of electrons in the electrode. (c) Illustration of redox-active cation intercalation, as seen in sodium hexacyanoferrate (NiHCF) electrodes with a cage-like lattice. (d) Intercalation through electrostatic interaction between intercalant and host material as seen in MXene electrodes.

(M)CDI [21] or by surface modification of carbon electrodes [22,23]. The use of intercalation materials is another approach to obtain a high charge efficiency without requiring membranes or surface modification, which reduces the complexity of cell design and electrode preparation.

In intercalation materials, the mechanism of ion storage via insertion into the interstitial lattice sites is different from that for carbon electrodes. In most types of intercalation materials, only cations or anions are adsorbed, and thus the co-ion expulsion effect is avoided leading to an enhanced charge efficiency of desalination. In addition, the use of intercalation materials facilitates size-based selective separation of ions with a certain valence and charge [24]. In contrast, porous carbon electrodes demonstrate a limited selectivity towards different ions [25–31]. As a substitute to the carbon electrode in CDI, intercalation materials have now been successfully employed as porous electrodes in a CDI cell setup [32–34].

A schematic picture illustrating an operational CDI cell with an intercalation material as an electrode is shown in Fig. 1(a). It depicts a flow-by configuration in which the electrolyte flows parallel to the porous electrode in an adjacent flow channel [35]. Fig. 1 represents a moment in time when cations intercalate into the cathode. This process can be controlled by the application of a current or voltage difference across the electrodes. As a consequence of cation intercalation, the salt concentration in the flow channel adjacent to the electrode decreases. Electrode regeneration can be easily accomplished by reversing the electrical current. Different configurations with an altered placement of the flow channel have also been explored [36]. The inset (b) in Fig. 1 represents the ion storage mechanism of intercalation electrodes. The

cation and an electron are included into the intercalation material to preserve the overall electroneutrality. A closer look into this mechanism is provided in the insets (c) and (d) that describe different types of intercalation material. In Fig. 1(c) a cation is inserted into a lattice vacancy while one of the lattice atoms is reduced [37], whereas in Fig. 1(d) cations intercalate in between the negatively polarized sheets of a layered structure [38].

A specific example of ion-intercalation followed by a redox reaction is observed in electrodes prepared from Prussian Blue (PB) and its analogues (PBAs) [39]. These materials (in their reduced form) generally have an ideal formula of $A_2M[Fe(CN)_6]$ where A is an alkali metal (Na, K). For PB, the element M is Fe whereas for PBAs, M can be Ni, Cu, Mn and other transition metal elements [40]. Upon (de)intercalation of a cation into/out of the interstitial site, the carbon-coordinated Fe undergoes a corresponding redox transformation, as shown in Fig. 1(b), and it ensures an electroneutral environment for the lattice. PBAs, which resemble zeolites in their structure, have crystal lattices with fixed dimensions (e.g., the diameter, d, of the entrance to the interstitial site in the PBA NiHCF is $d = 1.6\,\text{Å}$ [41]), and can filter out ions with a size that is above this diameter, making the electrodes ion-selective [42].

Another method of intercalation, as illustrated in Fig. 1(d), is observed with materials such as MXene. These are transition metal carbides, nitrides and carbonitrides (MXene phases) which are 2-D materials of the form $Ti_3C_2T_x$ (where T refers to a surface-terminated group such as O, OH or F) with layered structures. Ions of different size and valence have been demonstrated to intercalate in between such sheets

[38]. The ion storage in these materials is not necessarily accompanied by a redox reaction. However, it has been argued that in the case of Li intercalation, charge transfer occurs between the carbon atoms in the carbide sheets and the Li-ion [43].

Cation intercalation in the electrode, resulting in desalination, depends on the ion storage capacity of the electrode. If an electrode is perfectly selective to only adsorb either cations or anions, the ion storage capacity is directly proportional to the capacity to store charge, expressed in mAh/g. The utilization of this capacity depends on many factors, primary among them are the current density (in a constant current experiment [26]) and voltage (in a constant voltage experiment) and the salt concentration of the water. The operational conditions, dictated by these parameters, determine the actual realized charge capacity of the electrode as well as the retention of this capacity with number of cycles. In addition, these parameters influence the resistance in the cell and as a consequence, the rate of salt removal and the energy consumption in a desalination experiment [32,34]. An ideal CDI cell should have sufficient salt adsorption capacity, a high salt removal rate and low energy input.

This timeline overview attempts to chronicle the advances in the use of intercalation materials in the field of CDI, as briefly summarized in Fig. 2. In our view, this is an efficient method to map the progress in new electrode materials for CDI. We also include selected works about aqueous ion batteries that have had a direct consequence to the field of CDI. In the final section, we extrapolate from the literature and provide a brief outlook for future directions of research. Our work is intended to help in consolidating the efforts of the CDI community towards achieving improved solutions to selective and energy-efficient water desalination.

2. Timeline for intercalation materials in CDI

In this section we provide a chronological description of published studies that investigate the properties of intercalation materials (with and without redox activity) and employ these materials in a desalination process based on the principles of CDI. The order in which they are described here is determined by their date of submission, to provide an overview of how the field developed. Our descriptions are intended to give a clear picture of the idea behind every study, the reported observations, and the operational conditions.

To provide a better overview of each paper, keywords are also provided for each entry. The default system (which is *not* indicated with keywords) is as follows: the paper is an experimental study including data for the characterization of the electrode (three-electrode setup), and data of desalination in a CDI cell (two-electrode setup), with an aqueous electrolyte, and a single salt solution. Operation is asymmetric (anode and cathode have different composition) and there is no membrane. Deviations from this default system are addressed with keywords as listed in Table 1.

Besides these numerical keywords, information is provided on the mode of operation, i.e. constant voltage (CV) or constant current (CC), typical salt concentration, typical voltage or current, a specified value of salt adsorption capacity (SAC) in mg/g, and the electrode material, if not mentioned in the title of the paper.

1. Neff, V.D., 1978. Electrochemical Oxidation and Reduction of Thin Films of Prussian Blue. *Journal of the Electrochemical Society*. Kent state University, USA; *Submitted*: Sep. 29, 1977; *Revised*: Dec. 1, 1977 [37].

⇒ Keywords: (2)
This study demonstrated for the first time the electronic activity and redox properties of Prussian blue (PB). A 100 mM KCl solution was used as an electrolyte to perform cyclic voltammetry for thin film PB electrodes. The oxidation of the redox active center of the PB lattice with the applied potential was the cause of the reversible change in color of

the electrode film from blue to colorless. This hinted at the reversible nature of the redox reactions in the thin film electrode. It was the first evidence of cation intercalation in the interstitial sites of a PB lattice. The study was restricted to PB and did not investigate its derivatives (Prussian blue analogue, PBA).

2. Bocarsly, A.B. and Sinha, S., 1982. Effects of surface structure on electrode charge transfer properties: Induction of ion selectivity at the chemically derivatized interface. *Journal of Electroanalytical Chemistry and Interfacial Electrochemistry*. Princeton University, USA; *Received*: Aug. 17, 1982 [44].

⇒ Keywords: (2), (5), NiHCF
The capability of Nickel hexacyanoferrate (NiHCF) thin film electrodes to intercalate alkali metal cations is reported in this work. The experiments were performed for electrolytes of respective alkali metal ions, at a concentration of 1 M. The half-cell potential increased with increasing cation size following the trend $Li^+ > Na^+ > K^+ > Rb^+ > Cs^+$ in aqueous media. This implied that there was an inherent preference based on size towards the cations being inserted into the lattice of the thin film electrode. Fast (de)intercalation of Cs^+ ions against Li^+ ions was reported hinting clearly towards a size dependent affinity of the electrodes for the cations in a non-aqueous electrolyte. Works to follow would establish the size-based selectivity of PBAs towards different cations.

3. Schneemeyer, L.F., Spengler, S.E. and Murphy, D.W., 1985. Ion selectivity in nickel hexacyanoferrate films on electrode surfaces. *Inorganic Chemistry*. AT&T Bell Laboratories, USA; *Submitted*: Nov. 16, 1984; *Accepted*: Sep. 1985 [41].

⇒ Keywords: (2), (5)
This work made the first advance towards demonstrating the dependence of cation size on intercalation in NiHCF, a PBA. The authors identified the diameter of the interstitial site to be 3.6 Å and that of the lattice channel connecting this site, to be ~1.5 Å. Under the presence of an organic electrolyte, it was observed that Li^+ ions and Na^+ ions could intercalate reversibly but the insertion of K^+ ions was inhibited. The ions bigger than K^+, which are Rb^+ and n-tetra ethylammonium (TEA^+), did not intercalate at all. It was reported that a wider spectrum (in size) of cations was inserted into NiHCF in aqueous electrolyte and there was no clear size dependence trend, as seen for non-aqueous electrolytes. It was concluded that the role of water, in this departure from the observed trend of size selectivity in non-aqueous electrolyte is unclear.

4. Ikeshoji, T., 1986. Separation of Alkali Metal Ions by Intercalation into a Prussian Blue Electrode. *Journal of the Electrochemical Society*. Government Industrial Research Institute, Tohoku, Japan; *Submitted*: Nov. 16, 1984; *Accepted*: Sep. 1985 [24].

⇒ Keywords: (2), (5)
This work focuses on selective separation of alkali metal ions from an aqueous mixture of Li^+, Na^+, K^+, Rb^+, and Cs^+ ions by using $KFe_2[(CN)_6]$, a PB, as an electrode material. A platinum plate (area ~20 cm^2) with PB coatings on both sides was used to intercalate cations from a mixture in batch mode. The reduction steps were performed for a 100 mM ion solution for 10 min at a current of 1 mA. The regeneration step with alkali ion deintercalation was performed with a 100 mM acetic acid solution, giving rise to the effluent stream. It was reported that the total number of moles of cations removed was 95% of the total moles of charge input to reduce the oxidation state of the redox active iron in the PB lattice. The selectivity for the alkali metal cations, was reported to follow the order $Li^+ < < Na^+ < K^+ < Rb^+ < < Cs^+$. No explicit quantification of selectivity was provided but the mole fractions of the alkali ions in the effluent solution was reported as an
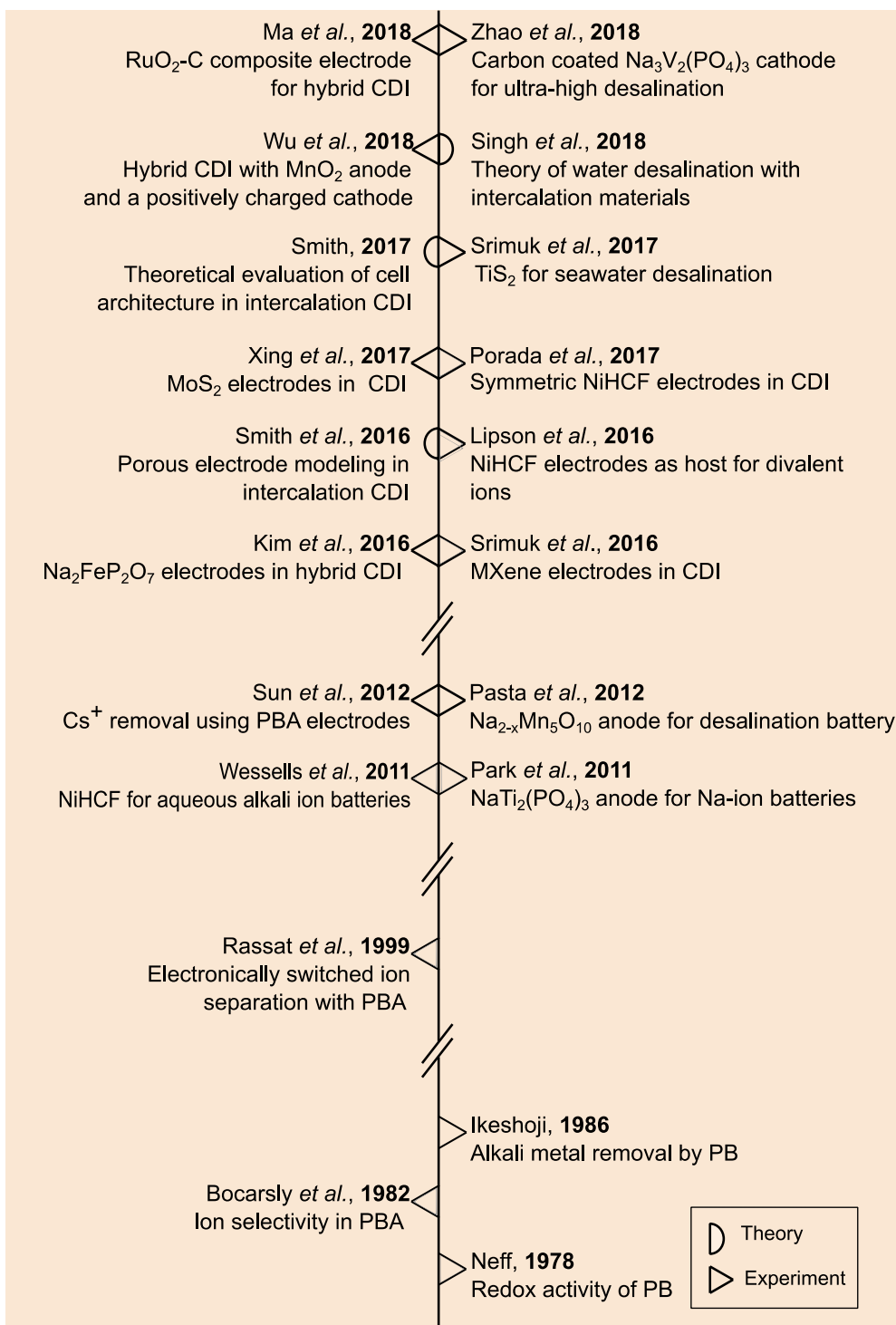
Ma *et al.*, **2018**
RuO$_2$-C composite electrode
for hybrid CDI

Zhao *et al.*, **2018**
Carbon coated Na$_3$V$_2$(PO$_4$)$_3$ cathode
for ultra-high desalination

Wu *et al.*, **2018**
Hybrid CDI with MnO$_2$ anode
and a positively charged cathode

Singh *et al.*, **2018**
Theory of water desalination with
intercalation materials

Smith, **2017**
Theoretical evaluation of cell
architecture in intercalation CDI

Srimuk *et al.*, **2017**
TiS$_2$ for seawater desalination

Xing *et al.*, **2017**
MoS$_2$ electrodes in CDI

Porada *et al.*, **2017**
Symmetric NiHCF electrodes in CDI

Smith *et al.*, **2016**
Porous electrode modeling in
intercalation CDI

Lipson *et al.*, **2016**
NiHCF electrodes as host for divalent
ions

Kim *et al.*, **2016**
Na$_2$FeP$_2$O$_7$ electrodes in hybrid CDI

Srimuk *et al.*, **2016**
MXene electrodes in CDI

Sun *et al.*, **2012**
Cs$^+$ removal using PBA electrodes

Pasta *et al.*, **2012**
Na$_{2-x}$Mn$_5$O$_{10}$ anode for desalination battery

Wessells *et al.*, **2011**
NiHCF for aqueous alkali ion batteries

Park *et al.*, **2011**
NaTi$_2$(PO$_4$)$_3$ anode for Na-ion batteries

Rassat *et al.*, **1999**
Electronically switched ion
separation with PBA

Ikeshoji, **1986**
Alkali metal removal by PB

Bocarsly *et al.*, **1982**
Ion selectivity in PBA

Neff, **1978**
Redox activity of PB

Theory

Experiment

Fig. 2. A brief chronology describing the development of intercalation materials based on selected papers.

indicator of the ion selectivity. This trend is opposite to what was observed in [44] for non-aqueous electrolytes. An inhibition of charge transfer due to the presence of Na$^+$ ions was observed during cyclic voltammetry of the PB film electrode in a K$^+$-Na$^+$ mixture. However, this observation was not explained.

5. Lilga, M.A., Orth, R.J., Sukamto, J.P.H., Haight, S.M. and Schwartz, D.T., 1997. Metal ion separations using electrically switched ion exchange. *Journal of the Electrochemical Society*. Pacific Northwest National Laboratory, USA; *Submitted*: Sep. 21, 1995; *Accepted*. Feb.

26, 1996 [45].

⇒ Keywords: (2), (5), NiHCF

This study describes the metal ion separation method defined as "Electrically switched ion-exchange" (ESIX). A thin film of nickel hexacyanoferrate (NiHCF), electro-deposited on a nickel surface, was studied for alkali metal ion insertion. It was demonstrated that the hexacyanoferrate film was selective towards Cs$^+$ in a Na$^+$ rich electrolyte. An earlier reported film fabrication procedure, carried out by applying a voltage of 1 V (vs. standard calomel electrode) to a nickel surface

Table 1
Keyword number and description, used to categorize all timeline entries.

Number	Description
1a	Only theory
1b	Theory and experiments combined
2	Only characterization in a 3-electrode setup; no desalination data
3	Symmetric operation, i.e. same chemical composition anode + cathode
4	Non-aqueous electrolyte
5	Solution with multiple ions
6	Including an ion-exchange membrane

exposed to 5 mM $K_3Fe(CN)_6$ and 100 mM KCl solution for 300 s, was modified to yield films of higher capacity and improved cycling rates. These modifications were termed as PNNL and were detailed in the work due to their proprietary source. During the discharge step, which is referred to as the load cycle by the authors, Cs ions were inserted into the NiHCF lattice. The charge step, referred to as unload cycle, leads to de-insertion of Cs^+ ions. The rate of diffusion of ions through the film was reported to be different for the charge and discharge steps. It was attributed to the solvent exchange process, but no further explanation was delivered. It was reported that the presence of Cs^+ ions in the interstitial sites of NiHCF made it stable in a highly basic medium. Based on previously observed trend of size dependent ion intercalation in PBA, as described in [37,44], the authors expected the Cs^+ ion to be the preferred cation for (de)insertion in NiHCF lattice from a mixture of multiple ions.

6. Rassat, S.D., Sukamto, J.H., Orth, R.J., Lilga, M.A. and Hallen, R.T., 1999. Development of an electrically switched ion exchange process for selective ion separatio. *Separation and Purification Technology*. Pacific Northwest National Laboratory, USA; *Submitted*: April 20, 1998; *Accepted*: July 15, 1998 [46].

⇒ Keywords: (2), (5), NiHCF
This work focuses on depositing an ion exchange film on an electrode surface followed by ion uptake into it and their subsequent elution. This is accomplished by changing the electrochemical potential of the deposited film. The film material used was NiHCF, a redox-active intercalation material. The improved film fabrication procedure from [45] was employed, leading to a higher capacity retention for the electrode. In addition, the authors attempted to quantify the selectivity of alkali-metal ions in pairs. The selectivity of K^+ and Cs^+ ions over Na^+ ions was systematically investigated for different salt mixture compositions using cyclic voltammetry (CV) and quartz crystal microbalance (for quantification of intake of ions by the NiHCF film). Very high selectivity ($\alpha_1^2 = \frac{x'_2 / x_1}{x_2 / x_1}$, where the numbers 1 & 2 serve as an identifier for the types of ions, x'_1 and x'_2 are mole fractions of ions 1 and 2 in the film; x_1 and x_2 are mole fractions of ions 1 and 2 in the bulk) was reported for Cs^+ ions over Na^+ ions for a salt solution with low (2300:1 Na^+:Cs^+ mole ratio) Cs^+ concentration. A sharp decrease in α was observed with an increase in the relative concentration of Cs^+ ions over Na^+ ions in the salt solution. It was argued that an estimation of separation factors was sensitive to the fluctuations in a apparent molar weights of pure species. A detailed discussion about the use of peak currents in a CV experiment for cation selectivity was also provided.

7. Yang, J., Zou, L., Song, H. and Hao, Z. 2011. Development of novel MnO_2/nanoporous carbon composite electrodes in capacitive deionization technology. *Desalination*. University of South Australia, Australia; *Submitted*: Feb. 24, 2011; *Accepted*: March 16, 2011 [47].

⇒ Keywords: CV, 1.2 V, 50 mM NaCl, 17 μmol/g-active material
This work uses MnO_2/nanoporous carbon composite for removal of

ions from brackish water using CDI. It was claimed by the authors that this was the first application of such a composite as an electrode for desalination purposes. Physical characterization revealed a smaller Brunauer–Emmett–Teller (BET) surface area (total surface area including micro and meso-pores) and pore volume, for the composite in comparison to the activated carbon. However, the meso-surface area (area of the meso-pores with size in between 2 and 50 nm) was found to be larger and was argued to be the effective area for desalination. Electrochemical characterization revealed a capacitive behavior with a rectangular voltammogram for the composite electrodes and in general, higher capacitance was reported for these electrodes compared to activated carbon. The authors claimed that MnO_2 can provide a high pseudo-capacitance. The desalination experiments were done at constant voltage and the electrochemical cell had only one flow channel, thus interrupting the supply of desalinated water during the regeneration step. The salt adsorption of the composite electrodes (17 μmol/g) was roughly three times the value observed for carbon electrodes (5 μmol/g), for a 50 mM NaCl solution and a maximum salt removal efficiency of ~81% was observed. The mechanisms for charge storage in MnO_2 were identified to be based on electrical double layer formation on pore surface, and intercalation of ion in the MnO_2 lattice followed by, as indicated by the authors, a faradaic reaction which must involve an electron transfer from the external circuit to the MnO_2 electrode. This may result in the change in the valence of the intercalated cation as specified in [48]. The contribution of each mechanism in the reported salt adsorption capacity of the composite electrodes were not specified or deliberated further.

8. Park, S.I., Gocheva, I., Okada, S. and Yamaki, J.I., 2011. Electrochemical Properties of $NaTi_2(PO_4)_3$ Anode for Rechargeable Aqueous Sodium-Ion Batteries. *Journal of the Electrochemical Society*. Kyushu University, Japan; *Submitted*: May 11, 2011; *Accepted*: June 17, 2011 [49].

⇒ Keywords: (4), (6)
This study reports on the use of $NaTi_2(PO_4)_3$ as anode material for sodium-ion batteries. Experiments were performed to ascertain the capacity of these anode materials in a Na_2SO_4 electrolyte. In addition, it was demonstrated that the loss of capacity of electrodes with charge/discharge cycle was higher for cells with aqueous electrolytes against those using organic electrolytes at low applied current densities. With increasing current density, the capacity retention for the electrode decays quicker in the organic electrolyte than aqueous electrolyte. In organic electrolyte, the electrodes lost ~70% of their initial capacity after 30 cycles at 20 A/m². In comparison, only 40% capacity loss was observed for aqueous electrolytes. A smaller over-potential for charge/discharge cycle was observed for aqueous electrolyte in comparison to organic electrolyte. The authors attributed this to the smaller impedance and viscosity in the aqueous medium. It was also observed that the decay in the capacity was accelerated at pH > 9 which was attributed to an easier decomposition of phosphate group in aqueous electrolyte. The authors identified the next step towards preparing a sodium ion battery is to find a Na^+ accepting electrode, stable in aqueous electrolyte.

9. Wessells, C.D., Peddada, S.V., Huggins, R.A. and Cui, Y., 2011. Nickel Hexacyanoferrate Nanoparticle Electrodes for Aqueous Sodium and Potassium Ion Batteries. *NanoLetters*. Stanford University, USA; *Submitted*: Sept. 13, 2011; *Accepted*: Nov. 01, 2011 [50].

⇒ Keywords: (2), (5)
This study demonstrates that NiHCF is an attractive material for grid-scale batteries due to its low cost, fast kinetics (because of its open framework structure) and long cycle life. The fabrication of NiHCF was carried out by a co-precipitation method where the reactants were

added dropwise to a common liquor to maintain a fixed reactant ratio and consequently, constant composition of the precipitate. The NiHCF electrodes were characterized in a three-electrode cell with NiHCF as a working electrode, an oversized NiHCF electrode as counter electrode Ag/AgCl electrode as a reference and aqueous 1 M solutions of NaNO$_3$ and KNO$_3$ as an electrolyte. The potential for insertion of Na$^+$ and K$^+$ into the NiHCF lattice was reported as 0.59 and 0.69 (vs. SHE).The capacity of NiHCF electrodes, for both the cations, was reported to be 60 mAh/g at a charging rate of C/6 (1C is the electrode charging rate at which the electrode is charged to its full, theoretical capacity in 1 h). The authors reported a capacity retention of 87 and 67% at charging rates of ~8C and 42C, respectively, in a NaNO$_3$ solution. A similar performance was observed when the cycling was performed in a KNO$_3$ solution. This led the authors to conclude that NiHCF can sustain high charge/discharge rates. The open framework structure, enabling fast ion diffusion, led to a low voltage hysteresis during cycling. An increase in the applied current density (and therefore the charging rate) resulted in a linear increase in voltage hysteresis. Most of this was attributed to the electrolytic resistance. The NiHCF electrode showed no capacity loss after 5000 cycles in the NaNO$_3$ solution sodium electrolyte at 8.3C. However, after 1000 cycles in the KNO$_3$ solution, capacity loss was observed. The authors also measured the effect of the state of charge on the NiHCF electrodes by ex-situ XRD spectra obtained for the electrodes at different states of charge. It was reported that the lattice parameters increased with charging (cation deintercalation) in the KNO$_3$ solution. This increase corresponded to an increase in the radius of [Fe^{2+}(CN)$_6$$^{3-}$] ion. The authors argued that the interaction of the so-called zeolitic water in the NiHCF lattice with water in the hydration shell of the (de)intercalating ions makes the transport process complex and less understood.

10. Pasta, M., Wessells, C.D., Cui, Y. and La Mantia, F., 2012. A Desalination Battery. *NanoLetters*. Stanford University, USA; *Submitted*: Nov. 4, 2011; *Accepted*: Jan. 23, 2012 [51].

⇒ Keywords: (5), CC, 5.0 A/m^2, seawater salinity, NaMNO

This study proposes a desalination battery for salt removal using a Na$_x$Mn$_5$O$_{10}$ (2 < x < 4 [13]) nanorod intercalation cathode and an Ag/AgCl anode. The desalination was performed in batch mode. The initial salt solution had a concentration equal to that of sea water and it was regularly changed after the cation uptake and removal half cycles. The NMO electrodes showed removal for ions other than Na$^+$ as well, notably Ca^{2+}, Mg^{2+} and K$^+$ ions. However, the K$^+$ ion was observed to be less preferred over other cations. The authors attributed this to the larger size of K$^+$ ions (without the hydration shell) in comparison to Ca^{2+}, Mg^{2+} and Na$^+$ ions. This finding is in contrast to what was reported in works before [24] and after this study [18] about the size of cation and their selectivity. The coulombic efficiency of the process was reported to be around 80% with the rest of the charge being diverted to side reactions such as the reduction of oxygen. The authors claimed that the efficiency values give information about the selectivity of the electrodes towards intercalating cations. Finally, energy values for the desalination battery and reverse osmosis were compared and it was found that the energy required for 25% reduction in salt concentration was 0.3 Wh/L, a value that, according to the authors, is comparable to that obtained for reverse-osmosis under similar conditions (0.2 Wh/L).

11. Lu, Y., Wang, L., Cheng, J. and Goodenough, J.B., 2012. Prussian blue: a new framework of electrode materials for sodium batteries. *Chemical Communications*. The University of Texas at Austin, USA; *Submitted*: March 10, 2012; *Accepted*: May 4, 2012 [15].

⇒ Keywords: (2)

This work is one of the first to indicate that PB and its analogues, prepared by replacing the Fe atoms in PB with transition metals such as Cu, Ni, Mn, Co, and Zn, can be a feasible electrode material for sodium-

ion batteries. From the X-ray diffraction characterization, it was concluded that different transition metal ions change the cubic lattice parameter. The electrochemical characterization was performed in an organic liquid carbonate electrolyte at a rate of C/20 (C is the current density in mA/g which can charge/discharge the electrode in an hour). The charge (deintercalation) capacity was reported to be higher than the discharge (intercalation) capacity for all the analogues. Insertion of Na$^+$ ions in KFe$_2$(CN)$_6$ showed a capacity of 100 mAh/g and the capacity remained stable for 30 cycles. The charge capacity declined with increasing number of cycles and plateaued at 120 mAh/g. It hints at the capacity of PB being higher than any of its analogues prepared by replacing Fe atoms with a transition metal element.

12. Sun, B., Hao, X.G., Wang, Z.D., Guan, G.Q., Zhang, Z.L., Li, Y.B. and Liu, S.B., 2012. Separation of low concentration of cesium ion from wastewater by electrochemically switched ion exchange method: Experimental adsorption kinetics analysis. *Journal of Hazardous Materials*. Taiyuan University of Technology, China; *Submitted*: May. 21, 2012; *Accepted*: July 3, 2012 [52].

⇒ Keywords: (3), (6), CV, 0–7 V, salinity 10–30 mg/L, NiHCF

NiHCF precipitated on porous three-dimensional carbon felt (PTCF) substrate is used in this work to remove Cs$^+$ ions from a salt solution in a continuous mode. The electrochemical cell comprised of two similar NiHCF electrodes separated by an AEM. The effect of variation in applied potential, salt concentration and pH were studied. Low concentrations of Cs$^+$ in the solutions, rarely encountered in literature (10–30 mg/L), were used to study cation adsorption. The removal of Cs$^+$ ions is reported to increase when the applied potential was increased from 0 to 7 V. Such high values of potentials are rarely seen in ion separation/removal studies involving redox-active electrodes and in CDI with aqueous salt solutions. Following the potentials, a variation in salt concentration resulted in no observable difference in the percentage adsorption of Cs$^+$ ions and a full 100% removal of Cs$^+$ ions was reported. A decrease in pH resulted in a decrease in the adsorption of Cs$^+$ ions. It was attributed to the increase in the concentration of H$_3$O$^+$ which may result in Cs$^+$ ions being repelled away from the electrodes, reducing their adsorption.

13. Chen, R., Tanaka, H., Kawamoto, T., Asai, M., Fukushima, C., Na, H., Kurihara, M., Watanabe, M., Arisaka, M. and Nankawa, T., 2013. Selective removal of cesium ions from wastewater using copper hexacyanoferrate nanofilms in an electrochemical system. *Electrochimica Acta*. National Institute of Advanced Industrial Science and Technology, Japan; *Submitted*: June 29, 2012; *Accepted*: Aug. 31, 2012 [53].

⇒ Keywords: (2), (5)

This study employs electrodes prepared by coating a titanium + gold substrate with copper hexacyanoferrate (CuHCF) to selectively remove Cs$^+$ ions from wastewater in a three-electrode cell. The Cs$^+$ ion removal was followed by regeneration of the electrode. The system was operated by switching the voltage between 0 and 1.3 V. A poor regeneration of active particles in the conventional system (using CuHCF powders in a Cs$^+$ solution), in comparison to the proposed three-electrode cell, was demonstrated. Metal removal was identified as a three step process. These steps were described as: bulk phase diffusion; film diffusion; and intra-particle diffusion. Diffusion in the particle, which the authors agreed was a slow process, was still not explicitly mentioned as the rate-limiting step. It was also claimed that the uptake capacity of the electrode decreased with an increase in electrode thickness due to active sites remaining unutilized. The removal efficiency however increased with increasing electrode thickness. This observation was attributed to an increase in surface area. Removal efficiency and uptake capacity saw no appreciable change in the pH range of 0–9. A sharp decline in these values was observed at a

pH of 12. A preference for Cs^+ over Na^+ ions was reported but no quantitative discussion was provided.

14. Lee, J., Kim, S., Kim, C. and Yoon, J., 2014. Hybrid capacitive deionization to enhance the desalination performance of capacitive techniques. *Energy & Environmental Science*. Seoul National University, South Korea; *Submitted*: July 28, 2014; *Accepted*: Aug. 28, 2014 [32].

⇒ Keywords: (6), CV, 1.2 V, 10–20 mM NaCl, SAC 31 mg/g-both electrodes, NMO

A novel hybrid desalination cell architecture is proposed in this work. The authors used $Na_4Mn_9O_{18}$ (NMO), a battery material, to fabricate a cathode and chose a porous carbon anode. The design includes a single channel for the flow of water. Consequently, there is no provision for a continuous supply of desalinated water. A high salt removal capacity of 31 mg was reported per grams of total electrode weight for a 10 & 20 mM salt solution when desalinated at a constant voltage of 1.2 V. The authors claimed this value to be twice as high as the one reported for conventional porous carbon CDI systems (i.e. ~14 mg/g). However, the exact operation conditions for the carbon electrodes used for comparison were not mentioned. In addition, the use of activated carbon as an anode material, which has a lower salt adsorption capacity than the NMO electrode was not a limiting factor in the desalination experiment. The ion-removal capacity was reported to remain constant with changes in salt concentration. The ion-removal rate and capacity increased with increasing applied voltage. It was attributed to the increase in the electro-sorption capacity of activated carbon electrode and an enhancement in the rate of reaction in the NMO electrode. The authors concluded that the proposed hybrid system can be used to desalinate water with high concentration (~100 mM).

15. Smith, K.C. and Dmello, R., 2016. Na-Ion Desalination (NID) Enabled by Na-Blocking Membranes and Symmetric Na-Intercalation: Porous-Electrode Modeling. *Journal of The Electrochemical Society*. University of Illinois at Urbana-Champaign, USA; *Submitted*: June 16, 2015; *Accepted*: Jan. 5, 2016 [36].

⇒ Keywords: (1a), (6), NiHCF

This study introduces a new electrochemical cell design for sodium ion desalination (NID). A precursor to this design has already been discussed in [54]. It presents a theoretical study of a symmetric cell with two similar intercalation electrodes used for desalination of a NaCl salt solution. The materials modeled in simulation were $NaTi_2(PO4)_3$ (NTP) and $Na_{0.44}MnO_2$ (NTP). A cell with an anion-exchange membrane and one with a non-selective membrane, separating the two electrode compartments, were compared for cation-removal performance. The equilibrium potentials for these electrode materials were estimated from their potentials against an Ag/AgCl reference electrode measured during a charge/discharge cycle. The study used the Butler-Volmer equation to model the current density because of cation intercalation into the redox-active electrodes. A modified expression for the exchange current density, derived from literature on the modeling of Li-ion batteries, was used with a dependence on electrolyte concentration and the intercalation degree of the electrodes. The current density obtained from the Butler Volmer equation was then used to model the time dependence of intercalation degree of the electroactive material in the electrode. A mass balance on the salt was written using Darcy's law for a flow through porous media with an additional term for the flux (in the form of current) due to (de)intercalation. The simulation results showed that the proposed cell can desalinate water of a salinity resembling seawater. It was concluded that ion selectivity in the separator membrane was essential for a high degree of desalination. It was also observed that increasing the applied current density increases polarization of electrodes leading to a rapid rise in voltage. The energy consumption was observed to decrease with increasing concentration

and decreasing electrode thickness.

16. Chen, R., Tanaka, H., Kawamoto, T., Wang, J. and Zhang, Y., 2017. Battery-type column for cesium ions separation using electroactive film of copper hexacyanoferrate nanoparticles. *Separation and Purification Technology*. University of Chinese Academy of Sciences, China; *Submitted*: Aug. 10, 2015; *Accepted*: Sep. 10, 2016 [55].

⇒ Keywords: (2)

The authors in this work propose a device for electrochemical removal of Cs^+ ions, referred to as battery-type column. The electrodes used for cation removal were fabricated by depositing CuHCF nanoparticles on a stainless-steel electrode through spray coating. The battery setup consisted of a platinum reference electrode, CuHCF nanoparticle coated stainless steel as the working electrode and a stainless-steel sheet as a counter electrode, like a three-electrode cell setup. Two different salt concentrations for Cs^+ ions were tested (4 and 6 ppm) and the removal efficiency in both cases was reported around 97%. The voltage was switched between 0 and 0.4 V to adsorb and desorb Cs^+ ions into the redox-active electrode. The kinetics of the redox reaction was divided in two parts and fitted with a pseudo-first and second order model. The authors argue that the Cs^+ ion removal is dominated by electro-static attraction in the initial stages of the reaction and gradually, as the opposite charge of the electrode is compensated, chemical reduction of Fe(III) to Fe(II) becomes the dominant cation removal mechanism. The reduction of iron in the beginning of the experiment was not considered. A stability analysis for the CuHCF film was performed by CV. The oxidation and reduction peaks were shifted away from each other and towards higher potentials. However, the changes were not discussed quantitatively further.

17. Chen, B., Wang, Y., Chang, Z., Wang, X., Li, M., Liu, X., Zhang, L. and Wu, Y., 2016. Enhanced capacitive desalination of MnO_2 by forming composite with multi-walled carbon nanotubes. *RSC Advances*. Fudan University, China; *Submitted*: Dec. 11, 2015; *Accepted*: Jan. 4, 2016 [56].

⇒ Keywords: CV, 1.4–1.8 V, salinity 30 mg/L, SAC 7 mg/g-active material

The authors use an electrode fabricated out of a composite of a multi-walled carbon nanotubes and MnO_2 for water desalination. The electrode was referred as a capacitor in this study. Its performance was also compared to that of the electrode with only MnO_2. A physical characterization revealed an increase in surface area in the composite against the regular MnO_2. A higher capacitance for the composite was reported and this was attributed to an enhanced surface area of MnO_2 together with a reduced internal resistance. The desalination experiments were performed in batch-mode for a solution with 30 mg/L NaCl. Activated carbon was used as anode. The operation was performed at different voltages between 1.4 and 1.8 V. The salt removal was reported as ~ 7 mg/g-total active materials weight in both electrodes. This adsorption capacity was 4 times higher than that observed for electrodes made of only MnO_2. This led the authors to conclude that the modified MnO_2 electrodes can be considered in CDI.

18. Lipson, A.L., Han, S.D., Kim, S., Pan, B., Sa, N., Liao, C., Fister, T.T., Burrell, A.K., Vaughey, J.T. and Ingram, B.J., 2016. Nickel hexacyanoferrate, a versatile intercalation host for divalent ions from non-aqueous electrolytes. *Journal of Power Sources*. Argonne National Laboratory; USA, *Submitted*: Jan. 27, 2016; *Accepted*: June 5, 2016 [57].

⇒ Keywords: (2), (4), (5)

This study employs NiHCF based electrodes to remove divalent ions from non-aqueous electrolyte solutions. The capacity of the electrode when cycled with Ca^{2+}, Mg^{2+}, and Zn^{2+} ions was reported to be

around 50 mAh/g, similar to aqueous solutions with Na$^+$ ions. The capacity also varied with the number of cycles. For a solution with Mg^{2+} ions the capacity increased to 80 mAh/g with increasing number of cycles whereas in case of Ca^{2+} ions, the capacity declined with increasing number of cycles. The capacity for the solution with Zn^{2+} ions was reported to be constant with the number of cycles. During cyclic voltammetry experiments, Ca^{2+}, Mg^{2+}, and Zn^{2+} ions gave a redox potential of 2.9, 2.6 and 1.2 V, respectively. The Na:Fe content in the electrodes was measured using EDX. The ratio dropped from 0.6 to 0.2 following the charging of electrodes (Charging here is referred to as the process of removing Na$^+$ ions from the Prussian blue lattice by subjecting it to high positive voltages). The elemental composition of the electrodes was also measured during charging and discharging by energy-dispersive X-ray spectroscopy. An increase in the content of Ca^{2+}, Mg^{2+}, and Zn^{2+} ions was reported upon discharge (discharging is referred to the process of insertion of cations in the NiHCF lattice). The change in lattice structure was monitored using XRD. As the change in lattice parameter was < 1%, it was concluded that repeated cycling is unlikely to cause any mechanical degradation in the lattice structure.

19. Kim, S., Lee, J., Kim, C. and Yoon, J., 2016. Na$_2$FeP$_2$O$_7$ as a Novel Material for Hybrid Capacitive Deionization. *Electrochimica Acta*. Seoul National University, South Korea; *Submitted*: March 5, 2016; *Accepted*: April 11, 2016 [33].

⇒ Keywords: (6), CV, 0.9–1.5 V, 10–100 mM NaCl, SAC 30 mg/g-cathode

This study proposes a hybrid capacitive desalination system (HCDI) with Na$_2$FeP$_2$O$_7$ as the primary redox-active cathode material. It consisted of an electrochemical cell with one inlet, a redox-active cathode and an activated carbon anode with an anion-exchange membrane separating them. The system was operated under constant-voltage conditions. The salt solution was continuously pumped into the cell and the delivery of freshwater was interrupted during regeneration of the electrodes. The electro-chemical characterization comprised of CV and galvanostatic intermittent titration (GIT). The capacity of the cathode, observed during GIT at a charging rate of 0.5C, was 56 mAh/g. The salt adsorption capacity (SAC) of this HCDI system was reported at 30 mg/g- Na$_2$FeP$_2$O$_7$ electrode. Different salt concentrations (10, 50, and 100 mM) were tested for three different voltages (0.9, 1.2, and 1.5 V). The rate of deionization increased by 40% when the concentration was increased from 10 to 100 mM. This was attributed to the decrease in ionic resistance of the electrolyte solution. The HCDI system was claimed to have a higher SAC to the membrane capacitive deionization (MCDI) systems with symmetric carbon electrodes at low applied current densities. The difference in performance between these two systems decayed at higher current densities. Thus, the authors concluded that at high current densities, the HCDI system cannot utilize the available capacity of the Na$_2$FeP$_2$O$_7$ for desalination. Therefore, the operation parameters are crucial for the performance of the proposed HCDI system.

20. Srimuk, P., Kaasik, F., Krüner, B., Tolosa, A., Fleischmann, S., Jäckel, N., Tekeli, M.C., Aslan, M., Suss, M.E. and Presser, V., 2016. MXene as a novel intercalation-type pseudocapacitive cathode and anode for capacitive deionization. *Journal of Materials Chemistry A*. Saarland University, Germany; *Submitted*: Sep. 9, 2016; *Accepted*: Nov. 2, 2016 [58].

⇒ Keywords: (3), CV, 1.2 V, 5 mM NaCl, SAC 13 mg/g-active material

This study reports on a new intercalation electrode material, modeled along the lines of an ideal supercapacitor, for CDI. It was referred to as MXene and was used in the form of nanosheets to intercalate anions as well as cations. The MXene electrodes were prepared by first fabricating Ti$_3$AlC$_2$ (referred to as the MAX phase) and then treating it

with hydrofluoric acid. The electrode was directly cast on the separator used to isolate the anodic and the cathodic compartments, for CDI experiments. The authors point out that this work was the first to adopt such an electrode preparation method in CDI. The galvanostatic charge/discharge of MXene resembles to that of a capacitor due to a linear rise in voltage with current (and therefore, the charge input). The capacitance of MXene when compared to activated carbon electrodes, was attributed to the intercalation of ions in between the MXene sheets. The authors argue that this feature qualifies MXene as a pseudo-capacitor material. It was observed that the voltage is not evenly distributed between the cathode and the anode and as a result, the potential is shifted to negative values. This observation was explained by the presence of groups terminating in −OH, =O and −F on MXene surface giving it a negative static charge. The salt adsorption was reported as 13 mg/g-active material for a 5 mM salt solution during a constant voltage operation at 1.2 V. The average salt adsorption rate was reported to be 1 mg/g/min. The electrodes were observed to be highly stable over 30 cycles. The authors identify the ion (de)intercalation and oxidation of the sheets as two primary sources of the observed morphological changes in the MXene.

21. Smith, K.C., 2017. Theoretical evaluation of electrochemical cell architectures using cation intercalation electrodes for desalination. *Electrochimica Acta*. University of Illinois at Urbana-Champaign, USA; *Submitted*: Sep. 21, 2016; *Accepted*: Feb. 2, 2017 [59].

⇒ Keywords: (1a), (3), (6), NiHCF

This theoretical study reports on the performance of NiHCF electrodes for various electrochemical cell architectures. The author demonstrated that the NiHCF electrodes are capable of efficiently desalinating water with seawater level salinity. The model was set up in a manner similar to that in [36]. For this work, a thermodynamic factor (activity γ) was included in the existing model relating the ionic current in the electrolyte to, as proposed by the authors, intercalation reaction current density derived from the Butler-Volmer equation. The activity coefficient was included to account for the concentrated nature of the salt solution which marked the shift from dilute to concentrated solution treatment. Experimentally measured bulk diffusion coefficient of salt along with revised bulk ion conductivity for a concentrated solution was included in the model. This, as the author claimed, aided in explaining the electrode polarization due to ohmic resistance as well as concentration changes in salt water flowing through the cell. The simulations were done for three cell designs: A flow-through (FT) cell, in which the water flows through the electrodes; A flow-by (FB) cell, in which the water flows along the electrodes in a channel; and a membrane flow by (MFB) cell in which an extra cation exchange membrane (CEM) is introduced between the flow channel and the electrode. The simulation results showed the MFB cell, with polarization and cation intake capacity, was comparable to the FT cell and better than the FB cell. A decrease in the discharge capacity of the FB cell was attributed to an increased polarization, due to the absence of a CEM. The enhanced performance of the MFB was attributed to its ability to retain salt within the electrodes. A similar explanation, however not provided, can be expected for the flow through electrodes which have similar performance as the MFB and employ only one membrane. It was claimed that the concentration in the FB cell decreases over time as compared to the MFB cell in which the concentration remains constant at the same initial salinity level when averaged across the cell width. The study went further to claim that the NiHCF electrode can be used to desalinate a 700 mM stream in an electro-dialysis stack.

22. Xing, F., Li, T., Li, J., Zhu, H., Wang, N. and Cao, X., 2017. Chemically exfoliated MoS$_2$ for capacitive deionization of saline water. *Nano Energy*. National Center for Nanoscience and Technology, China; *Submitted*: Nov. 11, 2016; *Accepted*: Dec. 7, 2016 [60].

⇒ Keywords: (2)

Following a study showing that chemically exfoliated nanosheets of MoS$_2$ (ce-MoS$_2$) containing a high concentration of the so-called metallic 1 T phase can electrochemically intercalate a series of group 1 ions with extraordinary efficiency [61], Xing et al. explore these 2D materials for electrode fabrication to remove ions from wastewater through CDI. In more detail, a comparison between electrodes made from, what is referred to as bulk MoS$_2$, and ce-MoS$_2$ was formulated. The exfoliation was performed on the 2H phase MoS$_2$ to obtain ultrathin 1 T phase MoS$_2$ nanosheets. The phases and properties themselves were not detailed in the work but can be found in [61]. Salt solutions from 50 to 400 mM were desalinated using the ce-MoS$_2$ and bulk MoS$_2$ electrodes. The maximum salt adsorption capacity observed was ~9 mg/g for a 400 mM NaCl salt solution at 1.2 V. The weight used to normalize the SAC value was not explicitly mentioned. This was claimed to be the highest in comparison to a series of five selected carbon-based electrodes. The comparison was hindered by the fact that the exact conditions (salt concentration, applied voltage) for the carbon electrodes were not mentioned. Nevertheless, this work does show the potential of using 2D ce-MoS$_2$ in CDI. Considering the high mass and volume-specific CDI performance, the authors believe that the as-prepared multilayer 1 T phase ce-MoS2 nanosheets will be favorable for the miniaturization of commercial CDI device.

23. Lee, J., Kim, S., and Yoon, J., 2017. Rocking Chair Desalination Battery Based on Prussian Blue Electrodes. *ACS Omega*. Seoul National University, South Korea; *Submitted*: Dec. 19, 2016; *Accepted*: April 13, 2017 [34].

⇒ Keywords: (6), CC, 5 A/m^2, 500 mM NaCl, SAC 60 mg/g-both electrodes

This study focuses on desalinating high salinity water by CDI in a continuous manner using two PBA electrodes. The desalination cell consisted of nickel and iron hexacyanoferrate (Na$_2$Ni[Fe(CN)$_6$] and Na$_2$Fe[Fe(CN)$_6$]) separated by an anion exchange membrane. The system had an intake of water from two channels which ran parallel to the electrodes. This ensured that the cell always produced a desalinated stream during operation. The main mechanism of cation removal was via intercalation into the interstitial lattice sites of the PB electrodes. In this system, when one electrode intercalates (takes cations in), the other deintercalates (releases cations out). The anions move from the cation deficient compartment to the cation rich compartment through the anion exchange membrane. It was reported that for a 500 mM NaCl salt solution at 5 A/m^2, the SAC was 60 mg/g-both electrodes. This number represents the salt adsorbed during intercalation in both the channels in one desalination cycle, where one desalination cycle comprises of intercalation and deintercalation steps. In this study, sodium citrate was added in the precipitation reaction mixture during the preparation of PBA. It coordinates with the metal ions and then, releases them slowly from the complex for reaction with the hexacyanoferrate ions. This, in theory, leads to a slow and ordered crystallization. At the same time, it did not make a significant improvement in the capacity which was reported to be 56 mAh/g-active particles. Therefore, addition of citrate during precipitation did not enhance the capacity of the PBA electrodes. It was concluded that the development of a flow type reactor would lead to enhancement of water treatment capacity for the proposed rocking chair desalination technique.

24. Porada, S., Shrivastava, A., Bukowska, P., Biesheuvel, P.M. and Smith, K.C., 2017. Nickel Hexacyanoferrate Electrodes for Continuous Cation Intercalation Desalination of Brackish Water. *Electrochimica Acta*. University of Illinois at Urbana-Champaign, USA; *Submitted*: May 2, 2017; *Published*: Sep. 22, 2017 [18] (*Electrochimica Acta*) *Submitted*: Dec. 25, 2016; *Published*: Dec. 25, 2016 [62] (ArXiv.org).

⇒ Keywords: (1b), (3), (5), (6), CC, 1.4–2.8 A/m^2, 20 mM NaCl, SAC 34 mg/g-both electrodes

This study presents an electrochemical cell prepared using two similar NiHCF cathode and anode for desalination purposes. This symmetric cell architecture for ion separation was referred to as cation intercalation desalination (CID) and this work is the first experimental demonstration of such a system. Two similar NiHCF electrodes interfacing the current collector on one side and a flow channel on the other were separated by an anion exchange membrane. This enabled the system to desalinate during the charge and discharge steps in a continuous mode. The total charge intake capacity of these electrodes was determined to be ~ 60 mAh/g, using the galvanostatic intermittent titration (GIT) technique. The presence of water in the interstitial sites of NiHCF indicated by elemental analysis was identified by the authors as one of the causes behind low intercalation of Na$^+$ ions in the lattice. Differential capacitance (as done in [63]) calculated from the GIT data gave a peak value of 1000 F/g which was claimed to be tenfold higher than a conventional carbon electrode used in CDI. This implied that NiHCF based electrodes can store the same amount of charge as the carbon electrodes at one tenth of the voltage. The desalination experiments were performed for a 20 mM salt solution at 1.4 and 2.8 A/m^2 in a constant current mode of operation. Higher current densities were avoided as they result in an increase in concentration polarization for a given salinity. The highest SAC reported (for one half cycle) was 34 mg of NaCl per gram of both electrodes and was 2.5 times higher than that reported for carbon electrodes in CDI. The deviation of current efficiency (moles of salt removed per mole of charge input) form unity was partly attributed to side-reactions occurring at high overpotential. A mixture of K$^+$ and Na$^+$ ions was also fed to the cell. The inherent selective nature of the NiHCF electrodes was demonstrated. For an equimolar salt solution, K$^+$ adsorption was three times higher than of Na$^+$ ions.

25. Erinmwingbovo, C., Palagonia, M.S., Brogioli, D. and La Mantia, F., 2017. Intercalation Into a Prussian Blue Derivative from Solutions Containing Two Species of Cations. *ChemPhysChem*. University of Bremen, Germany; *Submitted*: Jan. 8, 2017; *Accepted*: Jan. 25, 2017 [63].

⇒ Keywords: (1b), (2), (5)

This work uses NiHCF in a mixed aqueous electrolyte solution to observe the (de)intercalation of ions and the corresponding potentials. The measurements were done in a three-electrode cell. NiHCF electrodes were chosen to be the counter and the working electrode with an Ag/AgCl reference. It was claimed that in a mixture of cations, separate potentials corresponding to (de)intercalation of each constituent ions are not necessarily observed. The potential for intercalation of cations into NiHCF was measured by galvanostatic cycling in respective electrolytes of Na$^+$, K$^+$, and NH$_4^+$ ions with the total ion concentration of 500 mM. The potentials obtained increased in the order Na$^+$ < K$^+$ < NH$_4^+$. It was argued that a more favorable intercalation process corresponded to a higher intercalation potential. The authors claimed that the cations present in the interstitial sites were completely exchanged with those from the solution during the repeated charging/discharging of the electrodes. Different experiments performed with mixtures of ions (with differing ratios) indicated a transition from an average potential (single peak) of one cation to a combined potential according to the respective concentrations. Upon changing the concentration, the intercalation potential shifted, quasi-logarithmically, from one value to another. A simplified model to predict the single peak potential, observed for a cation mixture, was also presented. In more detail, a simple lattice model which assumes no interaction between intercalated species was adopted as the starting point. It was extended for solutions containing a mixture of intercalating species. The calculations implied that during intercalation, both the cations in the mixture were inserted in a defined ratio which was proportional to the

concentration of cations in the solution. An expression for the average potential, in line to the one obtained from the simplified model, was calculated for a solution with two cations. The authors concluded, upon comparison of the model with experimental data that the values of single peak potentials were satisfactorily close to those reported in literature.

26. Nam, D.H. and Choi, K.S., 2017. Bismuth as a New Chloride-Storage Electrode Enabling the Construction of a Practical High Capacity Desalination Battery. *Journal of the American Chemical Society*. University of Wisconsin − Madison, USA; *Submitted*: Feb. 1, 2017; *Accepted*: Aug. 4, 2017 [64].

⇒ Keywords: CC, 10 A/m^2, 600 mM NaCl, SAC 80 mg/g-bismuth

This study presents bismuth foam electrodes as a prospective candidate for Cl$^-$ ion storage, to be coupled with the cation-accepting NaTi$_2$(PO$_4$)$_3$, for water desalination. The bismuth anode stores Cl$^-$ ion as BiOCl while the cathode stores Na$^+$ by intercalation. It was reported that the reduction kinetics of BiOCl to Bi were slower than the oxidation. It was observed that ~50% of the Bi electrode was electrochemically active. Based on this, the Cl$^-$ storage capacity was reported to be ~ 80 mg/g of Bi. The faradaic efficiency of Cl$^-$ adsorption was reported to be nearly 100% since there were no competing oxidation processes. The desalination experiments were carried out by coupling Bi and NaTi$_2$(PO$_4$)$_3$ electrodes with no separation. The salt solution was 600 mM NaCl and operation was carried out at a constant current density of 10 A/m^2. The reduction of BiOCl requires an energy input (or an overpotential) in 600 mM NaCl. To facilitate this process and reduce the energy input, a 70 mM HCl was used to regenerate the Bi electrode. The evolution of cell voltage with capacity was reported and it was concluded that the capacity of the cell remains constant up to 200 cycles.

27. Chen, F., Huang, Y., Guo, L., Ding, M. and Yang, H.Y., 2017. A dual-ion electrochemistry deionization system based on AgCl-Na$_{0.44}$MnO$_2$ electrodes. *Nanoscale*. University of Technology and Design, Singapore; *Submitted*: March 16, 2017; *Accepted*: June 2, 2017 [65].

⇒ Keywords: CC, 100 mA/g, salinity 890 mg/L NaCl, SAC 57 mg/g-active electrode

This work employs an Ag/AgCl and a sodium manganese oxide electrode Na$_{0.44}$MnO$_2$, (NMO) to prepare an electrochemical cell for water desalination. The Ag/AgCl electrode was used as a Cl$^-$ donor/acceptor and the NMO electrode was used to (de)intercalate cations. The cell architecture consisted of the electrodes separated by a flow channel. The adsorption step was initiated with Na$^+$ ions being adsorbed faradaically, as claimed by the authors, in NMO and Cl$^-$ ions doing the same in the Ag/AgCl electrode. The desorption step involves a current reversal which leads to Na$^+$ and Cl$^-$ ions being released from the respective electrodes resulting in their regeneration. The value for charge capacity for the NMO electrode was reported to be ~390C/g-active material (~ 110 mAh/g) at 100 mA/g current density. It was reduced to 260C/g (~ 70 mAh/g) after 30 cycles. The salt concentration was 890 mg/L (15 mM) and the recovery efficiency was reported to be approximately 100%. A maximum value of 57 mg/g was reported for SAC and was claimed to be higher than those from the conventional and hybrid CDI. It must be noted that the channel does not produce desalinated water continuously due to interruptions during the regeneration steps. The salt adsorption decreased with increasing number of cycles and eventually settled to a final value of 57 mg/g-active electrode at the lowest applied current density of 100 mA/g. This adsorption, and the charge efficiency, decreased with increasing current density.

28. Srimuk, P., Lee, J., Fleischmann, S., Choudhury, S., Jäckel, N., Zeiger, M., Kim, C., Aslan, M. and Presser, V., 2017. Faradaic

deionization of brackish and sea water via pseudocapacitive cation and anion intercalation into few-layered molybdenum disulfide. *Journal of Materials Chemistry A*. Saarland University, Germany; *Submitted*: April 10, 2017; *Accepted*: July 4, 2017 [66].

⇒ Keywords: (3), CV, 0.8 V, 5–500 mM NaCl, SAC 25 mg/g-both electrodes

Electrodes fabricated from molybdenum disulfide (as used in [60] for CDI) and carbon nanotubes (MoS$_2$-CNT) are used in this study to desalinate water of high salinities. The salt adsorption results from the indiscriminate (de)intercalation of anions as well as cations in the layered 2-D structure of MoS$_2$. A similar mechanism was highlighted for electrodes made out of MXene [58]. The desalination operation was performed in constant-voltage mode at 0.8 V and the regeneration was done at 0 V. The salt concentration varied from 5 mM to 500 mM. The CDI cell consisted of two electrodes separated by a porous membrane and the solution was introduced in the cell in a flow-by mode, also discussed in [36]. The salt adsorption capacity reported by the authors was normalized by the total weight of both the electrodes. It was argued that the pseudo-capacitive behavior of the MoS$_2$-CNT electrode was confirmed by the triangular galvanostatic charge/discharge cycles and the high specific capacitance of 200 F/g was primarily attributed to the charge storage by intercalation into the MoS$_2$ sheets. An in-situ Raman spectroscopy analysis revealed that the ion insertion into MoS$_2$ expands the structure because the ions are bigger than the inter-layer spacing. The SAC value was reported to increase with salt concentration and the largest value of 25 mg/g-both electrodes was reported for a salt concentration of 500 mM and a constant voltage of 0.8 V. This was claimed to be higher than electrodes prepared from activated carbon only. Charge efficiency varied from 80% (for 5 mM salt concentration) to 95% (for 500 mM). The authors acknowledged the difficulty in comparison of different SAC values due to differing weights used for normalization. It was suggested to use the skeletal density of the materials to get around this problem.

29. Kim, S., Yoon, H., Shin, D., Lee, J. and Yoon, J., 2017. Electrochemical selective ion separation in capacitive deionization with sodium manganese oxide. *Journal of colloid and interface science*. Seoul National University, South Korea; *Submitted*: May 6, 2017; *Accepted*: July 16, 2017 [67].

⇒ Keywords: (5), CC, 10 mA/g, salinity 30 mM

This study deals with selective removal of ions from a mixed salt solution by using manganese oxide, an intercalation material, in CDI. The electrodes made from Na$_{0.44}$MnO$_2$ (NMO) were used in aqueous mixtures of Na$^+$, K$^+$, Mg^{2+}, and Ca^{2+} ions to selectively absorb Na$^+$ ions. The electrochemical cell consisted of Na$_{0.44}$MnO$_2$ cathode and an Ag/AgCl anode. The authors describe the salt removal process in two steps. The first one, the capture step is identified as the one during which, a pretreated NMO cathode intercalates cations from a 30 mM mixture of NaCl, KCl, MgCl$_2$, and CaCl$_2$ while the Ag/AgCl anode reacts with the Cl$^-$ ions. In the second one, the release step, the intercalated ions get released into a 30 mM LiCl solution, marking the regeneration of the cathode. The operation was performed under constant-current conditions. It was claimed that 49–57% of the charge was used to release and capture Na$^+$ ions in contrast to 35–37% involved for the divalent cations. Only 5% of the charge went towards capturing and releasing K$^+$ ions. Therefore, the selectivity towards Na$^+$ ions was reported to be 13 times higher than that for K$^+$ ions and 6–8 times higher than that for Mg^{2+} and Ca^{2+} ions. A preference towards Na$^+$ ions by NMO was inferred from the selectivity numbers and the cyclic voltammetry experiments which showed peak currents for Na$^+$ (de)intercalation into the cathode. A reason for such a preference was not provided.

30. Guo, L., Mo, R., Shi, W., Huang, Y., Leong, Z.Y., Ding, M., Chen, F.

and Yang, H.Y., 2017. A Prussian blue anode for high performance electrochemical deionization promoted by the faradaic mechanism. *Nanoscale*. Singapore University of Technology and Design, Singapore; *Submitted*: May 19, 2017; *Accepted*: July 30, 2017 [68].

⇒ Keywords: (6), CC, 125–1250 mA/g, salinity 10–200 mM NaCl, SAC 120 mg/g-active material

This study uses a hybrid (asymmetric) configuration with one activated carbon electrode and one based on pure PB particles ($Na_xFe_2(CN)_6$) in combination with both an anion exchange membrane and cation exchange membrane. The detailed chemical synthesis of the composite electrode, also containing graphene oxide, binder, and carbon black, was described. The PB forms nanocubes of about 200 nm size. In the 3-electrode experiment, cyclic voltammetry (CV) was used as well as galvanostatic charge/discharge. In CV, redox peaks at $+0.15/+0.05$ V vs Ag/AgCl, show relate to Na^+ (de)intercalation. In the CDI experiment, the current was varied between 125 and 1250 mA/g resulting in a cell voltage ranging between -1.4 V to $+1.4$ V. Salt concentration was in the range of 10–200 mM. A schematic was provided explaining the charge/discharge cycle, and ion adsorption/desorption in CDI with PB and activated carbon. Removal capacity was shown to be stable at ~40 mg/g up to 600 cycles. A maximum SAC of 120 mg/g was reported.

31. Yoon, H., Lee, J., Kim, S. and Yoon, J., 2018. Electrochemical sodium ion impurity removal system for producing high purity KCl. *Hydrometallurgy*. Seoul National university, S. Korea; *Submitted*: May 29, 2017; *Accepted*: Dec. 20, 2017 [69].

⇒ Keywords: (5), CC, 3 A/m^2, salinity 20–40 mM NaCl, KCl, KFeHCF, NMO

This study presents an electrochemical system comprised of $NaMnO_2$ and $K(Fe[CN_6])$ (KFeHCF) electrodes to selectively remove sodium impurities from a KCl solution to produce KOH of high purity. Two target solutions were used as feed: the first one consisted of 20 mM NaCl and 40 mM KCl and the second one contained 20 mM NaCl in 4 M KCl solution, replicating industrially relevant conditions. The impurity removal was done in four steps. In the first step, the electrochemical cell with a completely deintercalated NMO electrode and a fully intercalated KFeHCF electrode was operated in a constant current mode, such that the NMO electrode (cathode) intercalated ions from the target solution. Concomitantly, the anode deintercalates K^+ ions in the feed. In the second step, the feed solution was replaced with a 20 mM KCl solution to prepare for the regeneration of NMO electrode. In the third step, the direction of the applied current was reversed to regenerate the NMO electrode (anode). In the fourth and final step, the feed was replaced with the target solution. This completes one (four-step) cycle of operation. After the first step, the concentration of Na^+ ions in the target solution decreased by ~20% with a charge efficiency of ~76%. The efficiency reduced to 54% for the feed solution containing 4 M KCl. This difference was attributed to the interference from K^+ ions in the electrolyte. Next to this decrease in the Na^+ ion concentration, K^+ ions increased in the solution by ~12% due to deintercalation at the anode. Despite the decreased efficiency, the authors claimed that the NMO/ KFeHCF system was capable of removing Na^+ impurities from industry grade KCl solutions as ~36% of Na^+ ions were removed from it after three full cycles (12 steps).

32. Byles, B.W., Cullen, D.A., More, K.L. and Pomerantseva, E., 2018. Tunnel structured manganese oxide nanowires as redox active electrodes for hybrid capacitive deionization. *Nano Energy*. Drexel University, USA; *Submitted*: June 7, 2017; *Accepted*: Dec.10, 2017 [70].

⇒ Keywords: (5), (6), CV, 1.2 V, salinity 15 mM KCl, SAC 44 mg/g-both electrodes

This work presents a hybrid CDI system comprised of a redox active MnO_2 electrode paired with activated carbon in a flow-by cell configuration. The anode and the cathode were separated from the flow channel by an AEM and a CEM respectively. Four different types of MnO_2 with different crystal structures were tested to find an appropriate electrode material. The tunnel structure of different MnO_2 materials was found to be stabilized by different cations. These stabilizing cations were reported to facilitate repeated (de)insertion of cations from the feed solution. The CDI operation was performed under constant voltage of ± 1.2 V in batch mode for a 15 mM individual solution of Na^+, K^+ and Mg^{2+} ions. The MnO_2 phase with the most diverse tunnel sizes demonstrated the maximum SAC in NaCl (28 mg/g), KCl (44 mg/g) and $MgCl_2$ (43 mg/g). This led the authors to conclude that the structure with larger tunnels had higher capacity for ion storage. The relation between the salt removal and the tunnel size is not straight forward as the stabilizing ions were also reported to play a role in ion storage. The ion removal, which is linked to the reduction of Mn atoms, is reduced by the stabilizing ions may also partially reduce the oxidation states of Mn in the lattice. The charge efficiency was reported to be above 80% for each tested material. The ion removal by the MnO_2 electrodes was attributed to two mechanisms: First was the pseudo-capacitive adsorption of cations on the surface of the MnO_2 electrode; second was the diffusion controlled ion intercalation of ions in the crystal structure of MnO_2 electrode. The fast pseudo-capacitive adsorption of ions is followed by the slow intercalation into the MnO_2 lattice. This work successfully demonstrated the application of different MnO_2 electrodes for hybrid CDI.

33. Lee, J., Srimuk, P., Aristizabal, K., Kim, C., Choudhury, S., Nah, Y.C., Mücklich, F. and Presser, V., 2017. Pseudocapacitive Desalination of Brackish Water and Seawater with Vanadium-Pentoxide-Decorated Multiwalled Carbon Nanotubes. *ChemSusChem*. Saarland University, Germany; *Submitted*: July 5, 2017; *Accepted*: July 25, 2017 [71].

⇒ Keywords: CC, 33 mA/g, salinity 600 mM NaCl, SAC 24 mg/g-both electrodes

This study uses a multiwalled carbon nanotube (MWCNT) electrode, modified with vanadium pentaoxide (h-V_2O_5) to store Na^+ via pseudocapacitive intercalation. The electrochemical cell also consisted of an activated carbon electrode (AC) which was used to store Cl^- ions via electrosorption in the pores. The capacity of the MWCNT-hV_2O_5 electrodes was estimated to be ~ 45 mAh/g. The mass of AC electrode was twice that of the MWCNT-hV_2O_5 electrode because of the low capacity of AC. The desalination operation was performed at a constant current of ~33 mA/g-both electrodes for 200 and 600 mM salt solution. The SAC for a 200 mM NaCl solution was reported to be ~23 mg/g-both electrodes. The authors claimed that the high SAC value resulted from Na^+ ion intercalation into the hV_2O_5 electrode. A decrease in the SAC value with increasing number of cycles was attributed to structural degradation of V_2O_5. The SAC for a 600 mM NaCl solution was reported to be ~24 mg/g-both electrodes. The energy consumption value, reported for the 200 and 600 mM NaCl solution, were claimed to be lower than that for a MCDI cell. Finally, the study introduced another method for normalizing the SAC values to make a fair comparison between different electrode materials. The authors argue that the weight of the electrode adsorbing Na^+ ions should be used to normalize the salt removal capacity in the cell since it is the Na^+ removal which drives the whole process. This line of argument is applicable for systems with different materials for cathode and anode.

34. Srimuk, P., Lee, J., Tolosa, A., Kim, C., Aslan, M. and Presser, V., 2017. Titanium Disulfide: A Promising Low-Dimensional Electrode Material for Sodium Ion Intercalation for Seawater Desalination. *Chemistry of Materials*. Saarland University, Germany; *Submitted*: Aug.8, 2017; *Accepted*: Nov. 11, 2017 [72].

⇒ Keywords: CC, 0.1 A/g, 5–600 mM NaCl, SAC 14 mg/g-both electrodes

This work focuses on a composite electrode fabricated by blending titanium disulfide (TiS$_2$) with carbon nanotubes (CNTs) to desalinate water of high salinity. The 2-D layered structure of TiS$_2$ facilitates cation intercalation between the layers. The electrodes were prepared without the addition of a polymeric binder. Electrochemical characterization was performed in a standard three-electrode cell configuration through cyclic voltammetry (CV) and GIT. The desalination experiments were done in a conventional two-electrode CDI configuration. The TiS$_2$-CNT electrode was paired with a carbon electrode in a flow-by cell configuration, as illustrated in Fig. 1(a). The electrodes were separated by a porous separator. No IEM was employed in this cell setup. The experiments were performed at a single flow rate for 5, 50 and 600 mM NaCl solution. The salt removal was done at a constant current of 0.1 A/g in the potential window of 0.2–0.8 V. The TiS$_2$-CNT composite electrode exhibited a charge storage capacity of 68 mAh/g which was higher than the capacity observed for a pristine TiS$_2$ electrode (40 mAh/g). This was attributed to the addition of CNTs, which would provide a highly conducting network for ion (de)intercalation. The TiS$_2$-CNT electrodes were reported to suffer from poor capacity retention at voltages lower than −0.3 V. Repeated cycling at −0.4 V caused volume expansion, leading to an unraveling of the layered TiS$_2$ structure. The reason provided for the capacity decay at −0.6 V was change in phase from TiS$_2$ to TiO$_2$. During desalination experiments, the TiS$_2$-CNT//carbon cell exhibited a SAC value of ~11, 13 and 14 mg/g for a feed of 5, 50 and 600 mM NaCl, respectively. The charge efficiency of the process was reported to be in the range of 78–92%. The authors also argued to normalize the SAC values with the mass of the ion-selective electrode (TiS$_2$-CNT in this case) to give a fair assessment of the desalination performance of the electrode, because in a hybrid cell, the TiS$_2$-CNT electrode is paired with an electrode with low capacity. Therefore, normalization with the total electrode weight may not reflect the qualities of TiS$_2$-CNT composite electrode. This method resulted in a sodium ion removal capacity of 36 mg$_{(Na)}$/g$_{(negative\ electrode)}$.

35. Kim, T., Gorski, C.A. and Logan, B.E., 2017. Low Energy Desalination Using Battery Electrode Deionization. *Environmental Science & Technology Letters*. Pennsylvania State University, USA; *Submitted*: Sep. 3, 2017; *Accepted*: Sep. 18 2017 [26].

⇒ Keywords: (3), (6), CC, 3 A/m^2, 50 mM NaCl, SAC 100 mg/g-both electrodes, CuHCF

This study uses two copper hexacyanoferrate (CuHCF) electrodes in a symmetric electrochemical cell to remove cations from an aqueous 50 mM NaCl solution. The cell architecture allows for a desalinated and a concentrated stream being produced simultaneously. The authors refer to this technique as battery electrode deionization. The CuHCF are a type of PBAs and their electrodes store and release ions via (de)intercalation. The study introduced 1, 3, and 5 ion-exchange membranes (IEMs) between the electrodes and claimed that the difference in the feed and outlet concentration increased from 4 mM (in single stack cell containing only one IEM) to 12 mm (triple stacked, containing 5 IEMs). The maximum salt adsorption capacity reported was 100 mg-NaCl/g-electrodes for an applied current density of ~3 A/m^2. The authors report this number to be the highest yet in the CDI literature. The charge efficiency was reported around 80%. The salt adsorption capacity for a single-stacked cell was not provided. The authors also observed that only 60% of the full capacity of CuHCF was utilized. The total capacity was reported around 57 mAh/g-active material (205 C/g) when cycled in 1 M NaCl and 53 mAh/g-active material (205 C/g) when cycled in 50 mM NaCl electrolyte. The energy consumption with a triple-stacked cell was reported to be an order of magnitude lower than that observed in CDI and MCDI experiments for the same inlet and outlet concentrations. The authors concluded that the addition of extra

membranes reduced the energy consumption by ~30%.

36. Bao, W., Tang, X., Guo, X., Choi, S., Wang, C., Gogotsi, Y. and Wang, G., 2018. Porous Cryo-Dried MXene for Efficient Capacitive Deionization. *Joule*. Drexel University, USA; *Submitted*: Oct. 3, 2017; *Accepted*: Feb.16, 2018 [73].

⇒ Keywords: (3), CV, 1.2 V, 170 mM NaCl, SAC 45 mg/g

This work presents an enhanced porous MXene (Ti$_3$C$_2$T$_x$, T$_{xz}$(OH)$_x$O$_y$F$_z$) electrode, as used in [58] for CDI applications. The layered nanosheets of MXene were prevented from restacking, due to Van der Waals forces, by a vacuum freeze drying process to obtain an aerogel-like material. This led to the fabrication of a porous electrode with a large surface area (~290 m^2/g) in comparison to regular MXene electrodes (30 m^2/g). In addition, the porous MXene had larger pores in the range of 15–40 nm. The non-porous MXene lacked pores in this range. The authors speculated that this larger pore size gives sufficient space for the intercalation of Na$^+$ and Cl$^-$ ions. The porous MXene was electrochemically characterized through CV in a three-electrode cell configuration. The charge storage capacity was found to be 156 F/g, which was twice as high as the value reported for untreated MXene. The CDI cell prepared using the porous MXene electrodes exhibited a SAC value of 45 mg/g for a 170 mM NaCl solution under an applied voltage of 1.2 V. We note that the SAC normalization weight was not explicitly mentioned. The ion storage was attributed to a combination of EDL formation on the nanosheets of exfoliated MXene and the intercalation of ions in between the sheets, along the lines reported by Srimuk et al. [58].

37. Wu, T., Wang, G., Wang, S., Zhan, F., Fu, Y., Qiao, H. and Qiu, J., 2018. Highly Stable Hybrid Capacitive Deionization with a MnO$_2$ Anode and a Positively Charged Cathode. *Environmental Science & Technology Letters*. Dalian University of Technology, China; *Submitted*: Nov. 30, 2017; *Accepted*: Jan. 22, 2018 [74].

⇒ Keywords: CV, 1.4 V, 8 mM NaCl, SAC 14 mg/g-both electrodes

This work uses a cation-selective MnO$_2$ anode coupled with anion-selective quaternized poly-(4-vinylpyridine)-coated activated carbon cathode in a CDI cell setup not separated by an ion-exchange membrane. The intercalation of Na$^+$ ions was reported into the MnO$_2$ structure by the means of a reduction reaction and its oxidation would follow deintercalation of Na$^+$ ions during the charging step. The salt adsorption capacity of the cell with MnO$_2$ electrode was reported to be 14 mg/g-both electrode for a ~8 mM solution desalinated at 1.4 V. The SAC values were shown to increase upon increasing the applied voltage. In addition, it was demonstrated that these values were higher than those observed for the cell made of only carbon electrodes (10 mg/g). A decrease in charge efficiency was observed for an increasing applied voltage and it was attributed to an increase in the parasitic reactions in the cell. It was also argued that a higher amount of charge was consumed in the parasitic reactions during the charging step resulting in a higher charge efficiency for discharging step. A cyclic performance step revealed that the cell with MnO$_2$ anode retained a higher percentage of SAC after 350 cycles in comparison to the cell with both electrodes made from carbon. The improvement in the cyclic stability of the MnO$_2$ cell was attributed to the elimination of the carbon oxidation reactions prevalent in the cell with carbon anode.

38. Liu, S. and Smith, K.C., 2018. Quantifying the trade-offs between energy consumption and salt removal rate in membrane-free cation intercalation desalination. *Electrochimica Acta*. University of Illinois at Urbana-Champaign, USA; *Submitted*: Dec. 15, 2017; *Accepted*: March 11, 2018 [75].

⇒ Keywords: (1a), (3), NiHCF

This theoretical study makes a two-dimensional numerical analysis

of symmetric CDI with PBA intercalation materials where water flows through the pores of the electrode (i.e. without a flow channel), with the two electrodes separated by a diaphragm, i.e. an uncharged porous layer. Performance was analysed in terms of ASAR for the rate of desalination, and ENAS for the energy to desalinate, and were related to the dimensionless Péclet number and Damköhler numbers which describe fluid flow in relation to the diffusional rates. The flow-through design was compared with calculation results from a flow-by and a flow-behind configuration (where the water flows either in between the electrode and the diaphragm, or on the backside of the electrode). Flow-through was found to have superior desalination performance because in this geometry, ions advected with the water, and ion transport was not limited by diffusion and migration. Regular solution theory was used to describe the electrosorption process into the intercalation material, while also analytical results were presented.

39. Marzak, P., Yun, J., Dorsel, A., Kriele, A., Gilles, R., Schneider, O. and Bandarenka, A.S., 2018. Electrodeposited $Na_2Ni[Fe(CN)_6]$ Thin-Film Cathodes Exposed to Simulated Aqueous Na-Ion Battery Conditions. *Journal of Physical Chemistry C*. Technical University of Munich, Germany; *Submitted*: Jan. 12, 2018; *Accepted*: April 4, 2018 [39].

⇒ Keywords: (2)

This study investigates an electrochemically deposited layer of NiHCF in aqueous and organic electrolytes to understand its degradation and propose a mechanism for it. The electrode film NiHCF was electrodeposited directly from the reactants and were used in a three-electrode cell setup with a platinum wire as counter electrode. The electrodes were characterized, during operation, by atomic force microscopy to identify any morphological changes in the NiHCF lattice due to (de)intercalation of Na^+ ion. It was concluded, from the images which showed no difference in the morphology after repeated cycling, that the mechanical degradation is not the factor behind the loss of electrochemical capacity of the film over a period of use. A chemical change in the active material in the form of oxidation of nickel, into its oxide NiO_x at high pH, was claimed to be the primary cause in loss of electrochemical capacity of the electrodes. A change in the color of the film, from goldish to blackish, provided a visual confirmation of nickel oxidation. A mechanism for this degradation was also suggested. According to the study, the OH^- ions are adsorbed at nickel sites. The reaction of OH^- with Ni atoms destabilizes the lattice and leads to the extraction of iron centers. The intercalation capacity of an electrode is proportional to the amount of Fe centers and therefore, their removal makes the electrode inactive towards intercalation.

40. Srimuk, P., Lee, J., Fleischmann, S., Aslan, M., Kim, C. and Presser, V., 2018. Potential-Dependent, Switchable Ion Selectivity in Aqueous Media Using Titanium Disulfide. *ChemSusChem*. Saarland University, Germany; *Submitted*: March 5, 2018; *Accepted*: May 1, 2018 [76].

⇒ Keywords: (3), (5)

Electrodes fabricated from a composite of titanium disulfide and carbon nanotubes (TiS_2-CNT) are used in this study to selectively remove Cs^+ ions from a salt solution containing Cs^+ and Mg^{2+} ions. CV revealed different potentials associated with intercalation of different ions. The highest potential was observed for Cs^+ ions and the lowest was seen for Mg^{2+} ions, indicating an inherent preference of the electrode towards Cs^+ ions. It was reported that the electrodes exhibited different potentials for different cation concentrations due to their dependence on the activity of the redox species. A linear trend suggesting an increase in redox potential, associated with (de)intercalation of different cations in the electrode, with concentration was reported. For a multi-cation system, the potentials for (de)intercalation were shifted from the values observed during operation with a single cation system.

The potential difference observed between Cs^+ and Mg^{2+} ions was ~140 mV which had shifted from an expected value of ~65 mV. Multi-cation systems such as these were also studied in [63].The authors argue that the change in potentials of Cs^+ and Mg^{2+} ions in a multi-cation system does not render the system unsuitable for selective ion removal. An applied potential of −200 mV was suggested as an appropriate operating potential. The authors concluded the study by identifying three regimes of electrode potentials (vs Ag/AgCl) in which removal pf one cation was preferred over the other. In the potential range of −220 to −390 mV (vs. Ag/AgCl), Mg^{2+} ions were preferred with a molar selectivity of ~30 against Cs^+ ions. In the potential range of −220 to −160 mV, TiS_2-CNT electrode showed a weak preference towards Mg^{2+} ions (molar selectivity ~6). Finally, in the potential range of −220 to +26 mV, Cs^+ ions were removed with a molar separation factor of ~2. It was therefore concluded that the potential applied to a TiS_2-CNT electrode can be manipulated to selectively remove cation of choice from a multi-cation mixture.

41. Singh, K., Bouwmeester, H.J.M., de Smet, L.C.P.M., Bazant, M.Z. and Biesheuvel, P.M., 2018. Theory of Water Desalination with Intercalation Materials. *Physical Review Applied*. Wageningen University, Netherlands; *Submitted*: March 22, 2018; *Accepted*: May 4, 2018 [35].

⇒ Keywords: (1a), (3), (6)

The authors present a mathematical model of water desalination for a complete electrochemical CDI cell, with two electrodes interfacing with two flow channels separated by an anion exchange membrane. The authors implement the Nernst-Planck (NP) equation for ion transport on a complete desalination cell by neglecting any transport limitation within the intercalation material and assuming a dilute electrolyte. The transport processes modeled were: diffusion and migration of ions through the pores of the electrode; ionic transport in the flow channels; ion transport across the membrane. In addition to the NP equation, a Frumkin isotherm was implemented to relate the difference in potential between the cations in the electrode and the electrolytic phase with the intercalation degree (i.e. the ratio of concentration of cation in the intercalation particle and the maximum cation concentration in the intercalation particle) and the concentration of cations in the local electrolyte. The transport in the membrane was also described by the NP equation by assuming that only diffusion and electromigration occur in the membrane. The simulations were performed in the same manner as a constant- current desalination experiment is executed. Concentration profiles for different times were provided for (de)intercalation steps. In addition, the variation in intercalation degree with time was also demonstrated. The authors argued that the same starting value of the intercalation degree of the modeled electrodes gave them a symmetric character in terms of desalination and energy consumption. Therefore, the actions of one electrode were mirrored in the other electrode. Consequently, the authors claimed that an authoritative labeling of these operations as charging and discharging step lacked a definite criterion. A prediction of cell voltage with time also hinted at the possibility of energy recovery.

42. Choi, S., Chang, B., Kim, S., Lee, J., Yoon, J. and Choi, J.W., 2018. Battery Electrode Materials with Omnivalent Cation Storage for Fast and Charge-Efficient Ion Removal of Asymmetric Capacitive Deionization. *Advanced Functional Materials*. Seoul National university, S. Korea; *Submitted*: April 19, 2018; *Accepted*: July 11, 2018 [77].

⇒ Keywords: (5); CV, 1.2 V, 500 mM salt mixture, SAC 20 mg/g-both electrodes, CuHCF

This study presents an IEM-free asymmetric CDI cell with a cathode fabricated out of a metal organic framework (MOF) and porous carbon anode. The MOF material used to fabricate an electrode was $K_{0.03}Cu[Fe$

(CN) $_6]_{0.65} \cdot 0.43H_2O$, which has a comparable structure to the previously observed PBAs [18,26]. The MOFs were mixed with carbon and a polymer binder. Electrochemical tests were performed in a three-electrode cell configuration through CV and GIT to assess the charge storage performance of the MOF-containing electrodes prior to their use in a two-electrode CDI cell with MOF cathode and an AC anode, MOF//AC. The electrochemical characterization and the desalination performance of the CDI cell was monitored in 1 M salt solutions of K^+, Na^+, Mg^{2+} and Ca^{2+} ions as well as a 4000 ppm (~68 mM) mixture of all the these cations. The desalination capacity of the MOF cell was tested at a constant applied voltage of 1.2 V. The authors concluded from the characterization experiments that the MOF-containing electrodes were capable of intercalating all the tested cations within the water stability window, from their individual solution and from their mixture. The charge storage capacity obtained for the cations during galvanostatic charging at 50C were 52, 45, 36 and 40 mAh/g, respectively for K^+, Na^+, Mg^{2+} and Ca^{2+}. The difference in the observed capacities can be understood from the difference between the sizes of the cations and consequently, their ion mobility in the solution. It was reported that AC//AC cell predominantly removed divalent ions from the mixture. The MOF//AC cell exhibited invariant intercalation for mono and divalent ions. However, K^+ and Na^+ were removed 70% and 26% more, respectively, than Mg^{2+}. The authors also noticed that intercalation of water molecules in association with the incoming cation from thermogravimetric analysis (TGA) of electrodes before and after complete discharge. The amount of intercalated water molecule was higher for divalent cations due to their strong electrostatic interaction with water molecules. A charge efficiency of 76% was obtained for a MOF//AC cell which was significantly higher than a AC//AC cell (33%) without an IEM. The MOF//AC cell exhibited a similar ion removal capacity of 20 mg/g in a 500 mM mixture of ions. This was higher than the SAC value obtained from the AC//AC cell (5 mg/g). It was concluded that the open framework structure of the MOF crystals facilitated fast ion kinetics leading to a rapid ion and charge transfer. This enhanced the salt-removal rate and made it possible to utilize the maximum of the charge storage capacity available.

43. Ma, X., Chen, Y.A., Zhou, K., Wu, P.C. and Hou, C.H., 2018, Enhanced desalination performance via mixed capacitive-Faradaic ion storage using RuO2-activated carbon composite electrodes. *Electrochimica Acta*. Xiamen University, China; *Submitted*: May 12, 2018; *Accepted*: October 29, 2018 [78].

⇒ Keywords: CV, 1.2 V, 5 mM NaCl, SAC 11 mg/g-both electrodes

This study deals with a composite of ruthenium oxide (RuO_2) and activated carbon to prepare a high-performance hybrid CDI electrochemical cell. A combination of electrostatic deposition of ions on an EDL and faradaic processes were claimed to participating mechanisms behind the salt removal by the proposed system. RuO_2 was electrodeposited on AC through CV to prepare the composite electrodes. The amount of deposited RuO_2, and hence also the specific surface area available for EDL electrodeposition of ions, was controlled by the number of deposition cycles in CV. This study advocates a balance between retaining the specific surface area of the composite electrode available from the CNTs and the amount of electrodeposited RuO_2 on the CNT surface to make the most out of the two participating storage mechanism. The study presents two sets of experiments. The first one utilizes a setup is a three-electrode cell used for electrochemical characterization of the RuO_2-AC electrode (working electrode) through CV and GIT in a potential range of -0.4 to 0.6 V. The second setup consisted of a desalination cell comprising of two electrodes separated by a spacer channel. A 5 mM feed solution was recirculated through the cell and the salt removal was performed at a constant voltage of 1.2 V. The electrode regeneration was performed by the short circuiting of electrodes. In the electrochemical characterization experiments, an enhanced charge/discharge cycle time for the composite electrode in

comparison to the regular AC electrodes indicated an increase in the storage capacity of the RuO_2-AC electrodes by the active RuO_2 particles. It was also claimed by the authors that the addition of RuO_2 facilitated electron transfer and therefore, reduced resistance of the electrode. The CV experiments for RUO_2-AC composite electrode yielded a higher charge storage capacity (60.6 F/g) than the AC electrodes (31.1 F/g). It was concluded that the deposited RuO_2 was active and can enhance the charge storage capacity of the electrode due to its pseudo-capacitance charge storage. The desalination experiments employed RuO_2-AC electrode as a cathode to remove Na^+ ions. The SAC obtained after operating the cell at 1.2 V for 1 h in a 5 mM NaCl solution is reported to be ~11 mg/g-electrodes. The relative contribution of the capacitive and faradaic salt adsorption by the electrodes was calculated as 18% and 82%, respectively. The charge efficiency of the RuO_2-AC//AC cell, at 60%, was reported to be higher than that of a regular AC//AC cell, at 27%. A tabulated summary was provided to demonstrate a superior performance of the RuO_2-AC electrodes in comparison to MnO_2 based composite electrodes. However, the exact redox reactions behind the claimed pseudo-capacitance of the composite electrodes were not provided.

44. Byles, B.W., Hayes-Oberst, B. and Pomerantseva, E., 2018. Ion Removal Performance, Structural/Compositional Dynamics, and Electrochemical Stability of Layered Manganese Oxide Electrodes in Hybrid Capacitive Deionization. *ACS Applied Materials & Interfaces*. Drexel University, USA; *Submitted*: June 10, 2018; *Accepted*: September 5, 2018 [79].

⇒ Keywords: (5), (6), CV, 1.2 V, 15 mM NaCl, SAC 31–50 mg/g-both electrodes

This work utilizes two-layered manganese oxides (LMOs) stabilized by hydrated Na^+ ions (Na-birnessite) and Mg^{2+} ions (Mg-buserite) in a HCDI cell configuration, similar to those reported in [32,33]. The difference in the structure of Na-birnessite and Mg-buserite arises from the structural water layers residing in between the layers with the stabilizing ions. The LMO electrodes, prepared by mixing the active materials with carbon black and poly(tetrafluoroethylene) (PTFE), were used as cathodes with activated carbon (AC) anodes. The electrodes were mounted in a HCDI cell with the flow channel separated from cathode and anode with a cation and an anion exchange membrane, respectively. The ion-adsorption was performed for two separate NaCl and $MgCl_2$ salt solutions (both 15 mM) in a constant voltage mode of operation. The SAC recorded within the first 10 adsorption/desorption cycles for a NaCl solution with Na-birnessite and Mg-buserite were 31.5 and 37.2 mg/g-total electrode weight, respectively. For a $MgCl_2$ salt solution, Na-birnessite and Mg-buserite demonstrated a SAC of 50.2 and 39 mg/g-total electrode weight. It is interesting to realize that both electrode materials removed higher amounts of NaCl than $MgCl_2$. This result was correlated to the larger size of hydrated Mg^{2+} ions in comparison to the size of Na^+ ions. In addition, it was also observed that HCDI cell with Mg-buserite delivered higher SAC values when operated in a NaCl solution. This was attributed to a higher interlayer spacing in the Mg-buserite. In contrast, the HCDI cell comprising of Na-birnessite, with smaller interlayer spacing, delivered higher SAC in $MgCl_2$ solution. This counter-intuitive observation could not be explained by the current study. Extended cycling revealed that the SAC reduced upon increasing number of cycles. In addition, the SAC retention for the NaCl solution was found to be higher than $MgCl_2$, which was rationalized by an easier diffusion of smaller and single charge carrying Na^+ ions in comparison to Mg^{2+} ions. It was claimed that the ion removal proceeded via surface adsorption and redox reaction with the electrode material itself. This was postulated based on EDX spectroscopy, which showed the presence of the stabilizing ion as well as the cation from the salt solution in the composition of the electrode. Therefore, the change in interlayer ion content and consequently, the interlayer spacing, were argued as significant factors to be considered for extended cycling of

HCDI cell with Na-birnessite and Mg-buserite electrodes and their SAC in desalination experiments.

45. Kim, T., Gorski, C.A. and Logan, B.E., 2018. Ammonium Removal from Domestic Wastewater Using Selective Battery Electrodes. *Environmental Science & Technology Letters*. Pennsylvania State University, USA; *Submitted*: July 2, 2018; *Accepted*: Aug. 2, 2018 [80].

⇒ Keywords: (5), (6), CV, 0.1–0.3 V, ion concentration 5 mM NH_4^+, 20 mM Na^+, CuHCF

An electrochemical cell assembled with two intercalation electrodes fabricated using CuHCF, a PBA, is used in this study to selectively remove NH_4^+ ions from a mixture of ions. The cell used the same materials for both the electrodes which were separated by an anion-exchange membrane. This was achieved by manipulating the applied voltage. Such treatment of a multi-cation salt solution has been described for TiS_2 electrodes in [76] and cyclic voltammetry has been used to demonstrate different potentials of intercalation in a CuHCF electrode for different ions [42]. Electrochemical analyses have demonstrated that various cations such as Li^+, Na^+, K^+, and NH_4^+ intercalate into PBAs, such as CuHCF, at different potentials. One of the studies reviewed here reported extensive observations on this phenomenon and attempted to support the experimental data of ion intercalation with a thermodynamic model [63]. It was proposed that the higher intercalation potential observed for NH_4^+ ions (vs. SHE) in comparison to that of Na^+ ions should result in its preferential adsorption. The electrodes used in this study were prepared by the method similar to that in [26]. Two salt solutions with varying and similar concentrations for NH_4^+ and Na^+ ions were treated to ascertain the selective removal performance of the cell. For the salt solution with NH_4^+ concentration of 5 mM and Na^+ concentration of 20 mM, an increase in the applied voltage from 0.1 V to 0.3 V increased the removal of NH_4^+ ions from 65 to 93%. However, an increase in voltage resulted in a decrease in the selectivity towards NH_4^+ ions, reflected by the decrease in the separation factor (i.e. % NH_4^+ removed/% Na^+ removed) from 6 to 2. Non-selective MnO_2 electrodes tested for the same salt concentration at 0.2 V were reported to show a separation factor < 2. The CuHCF electrodes produced a separation factor of ~3.The concentration of ions was varied and it was claimed that the selectivity increased upon increasing NH_4^+ concentration. The authors identified the operation potential of 0.2 V to be optimal for NH_4^+ ion removal (80%) and selectivity (separation factor ~3).

46. Shi, W., Zhou, X., Li, J., Meshot, E.R., Taylor, A.D., Hu, S., Kim, J.H., Elimelech, M. and Plata, D.L., 2018. High-Performance Capacitive Deionization via Manganese Oxide-Coated, Vertically Aligned Carbon Nanotubes. *Environmental Science & Technology Letters*. Yale University, USA; *Submitted*: July 31, 2018; *Accepted*: September 25, 2018 [81].

⇒ Keywords: CV, 1.2 V, 100 mg/L NaCl, SAC 28 mg/g-one electrode

This work focuses on the fabrication of MnO_2-coated, vertically aligned carbon nanotube (VACNTs) electrodes prepared via Atomic Layer Deposition (ALD) for capacitive deionization. The technique of ALD was chosen to deposit thin films of MnO_2 on the VACNTs in order to enhance their SAC while still retaining a high electronic conductivity. Two sets of experiments were performed to assess the performance of the composite electrode. The first was electrochemical characterization performed in a three-electrode cell configuration through CV. The second set of experiments were done to ascertain the salt removal performance of the electrode. A 100 mg/L (~1.8 mM) flow solution was recirculated, in a batch mode, through a two-electrode cell, with a VACNT-MnO_2 as cathode and AC as anode to study the salt removal at a constant voltage of 1.2 V. The electrochemical characterization yielded a charge storage capacity of 220 F/g for VACNT-MnO_2,

which was higher than that for uncoated VACNTs (53 F/g). This increase was attributed to the intercalation of alkali metal ions in the MnO_2 crystal lattice. The charge storage capacity of the cathode decreased upon increasing thickness of the MnO_2 coating. This was attributed to an increase in the ohmic resistance and reduced accessible functional area in the electrode, like the proposition made in [78]. The desalination experiments yielded an optimized SAC of 490 μmol/g-cathode (~28 mg/g-cathode), which is higher than the SAC obtained by using pristine VACNTs (~15 mg/g-cathode).

47. Zhao, W., Guo, L., Ding, M., Huang, Y. and Yang, H.Y., 2018. Ultrahigh Desalination Capacity Dual-ion Electrochemical Deionization Device Based on $Na_3V_2(PO_4)_3$@ C-AgCl Electrodes. *ACS Applied Materials & Interfaces*. Singapore University of Technology and Design, Singapore; *Submitted*: August 15, 2018; *Accepted*: Oct. 29, 2018 [82].

⇒ Keywords: (6), CC, 0.1–0.5 A/g, 1 g/L NaCl, SAC 98 mg/g-both electrodes

This work deals with $Na_3V_2(PO_4)_3$ (NVP) as a cathode material in a dual-ion electrochemical deionization (DEDI). The origin of the term dual is not specifically motivated. The authors claim that the electrode materials for EDI achieve high SAC values by participating in redox reactions with either sodium or chloride ions in the feed solution. The electrochemical cell proposed in this work uses carbon-coated NVP as a Na^+ faradaic electrode and Ag/AgCl as anode. Three different types of NVP structures were tested: sphere-, wire- and flower-shaped NVPs. The NVP-C electrodes were electrochemically characterized via cyclic voltammetry (CV). The desalination experiments were performed in an EDI cell with the cathode and anode separated from the flow channel by a CEM and an AEM, respectively. The feed contained 1000 mg/L NaCl (~18 mM) and the desalination step was performed by applying a constant current of 100–500 mA/g. The wire-shaped NVP exhibited a better SAC value and the removal rate was comparable to the other two NVP structures. At an applied current density of 100 mA/g, the SAC value observed for wire-shaped NVPs was 98 mg/g; in both cases after 50 cycles. Bare NVP, without any carbon coating exhibited a reduced capacity of 70 mg/g. The salt adsorption rates varied from 0.04 to 0.14 mg/g/s with increasing applied current. The SAC value was claimed to be higher than the values reported in literature using DEDI technology.

48. Agartan, L., Hayes-Oberst, B., Byles, B.W., Akuzum, B., Pomerantseva, E. and Kumbur, E.C., 2019. Influence of operating conditions and cathode parameters on desalination performance of hybrid CDI systems [83]. *Desalination*. Drexel University, USA; August 22, 2018; *Accepted*: October 31, 2018.

⇒ Keywords: (6), CV, 1.2 V, 10 mM NaCl, SAC 23–26 mg/g-both electrodes, NMO

This study reports on the effect of operation parameters like feed flow rate and half cycle time (time given to the system for ion (de) intercalation) and cathodic parameters like cathode thickness as well as the loading of a conductive additive on the salt removal performance of a hybrid CDI cell. A faradaic cathode, prepared from α-MnO_2 and a capacitive anode, prepared out of AC, were separated by an IEM to assemble a water desalination cell. Two salt removal mechanisms were suggested to be functional in the cathode namely, pseudo-capacitance and ion intercalation in the crystal structure of the α-MnO_2. The desalination performance of the cell was tested in experiments under constant voltage of ± 1.2 V in a batch mode with a 10 mM NaCl solution. To test the influence of each of the experimental parameters mentioned above, their values were systematically altered and the corresponding system response was recorded. The comparison between the salt adsorption rate (SAR) values obtained for the half cycle times 120 and 240 min made the authors to conclude that the electrode was

saturated after the 120 min cycle length and the salt removal had become diffusion controlled, leading to a decrease in the SAR. Increase in feed flow rate (from 5 mL/min to 40 mL/min) led to an increase in the SAC values (from 18 to 23 mg/g). This was attributed to a more effective ion transport to the electrodes at higher flow rates. Systematic increment in the electrode thickness (from 150 to 450 μm) resulted in an increase in the SAC of the electrode (from 23 to 26 mg/g). However, further increase in electrode thickness to 600 μm resulted in a SAC of 13 mg/g. This decrease was attributed to an increase in electronic resistance and increase in the diffusion path length in the electrode. These factors resulted in an incomplete utilization of the active material in the electrodes. Finally, an increase in the loading of the conductive additive (from 10 wt% to 50 wt%) to the electrode led to an increase in their SAC from 23 to 25 mg/g. This increase was observed even with a decreasing amount of active material in the electrode. The authors observed that the trends in salt removal performance of the composite electrode cell for electrode thickness and half cycle time aligned with the trends reported for CDI systems. However, those obtained for different flow rates and the loading of conductive additives were opposite of what has been observed in the CDI literature.

3. Insights

The timeline overview, presented in Section 2, gives a description of the main findings reported by the studies on intercalation electrode materials. To provide a better insight into the functioning of intercalation electrodes in CDI, we highlight recurring aspects that have been addressed in the studies related to the cell architecture (Section 3.1) and operation parameters (Section 3.2).

3.1. Cell architecture

The studies described in this work employed different architectures for the desalination cell in terms of the materials used to fabricate the cathode and the anode for ion adsorption. A CDI process can be performed with a two-electrode cell configuration where the electrodes may or may not be separated by an ion-selective membrane. However, several works reported here also used a three-electrode cell to characterize the intercalation electrodes. These papers are usually encountered very early in the timeline, when the properties of intercalation materials were not yet well understood [24,37], or when new avenues were being explored later [39,57,63]. The two-electrode cell configuration, relevant for desalination applications, can employ different types of cathodes and anodes. A common theme among these cell configurations is the use of intercalation materials as the positive electrode to adsorb cations. This adsorption is usually accompanied by the reduction of one of the lattice elements of the electrode material. An exception is the system reported in [58,84] where an indiscriminate ion adsorption occurs without a redox reaction.

Desalination cells consisting of a cathode and an anode with the same chemical composition with two flow channels on either side of an ion-exchange membrane, are referred to as *symmetric* cells, explored more than one decade ago in [54]. If operational conditions such as the water flow rate in the two channels are also symmetric, a symmetric cell leads to symmetric operation, where the processes in one compartment in one half of the cycle, are the same as in the other channel in the other half of the cycle, making the cell easy to operate [36].

An interesting point relevant for symmetric systems with intercalation electrodes, is that the desalination performance depends on the initial charge of the electrode. If for instance both electrodes are initially almost fully deintercalated (low concentration of adsorbed cations) and thus the redox-active atoms in the lattice almost fully oxidized, the cycle will be far from optimal, because quickly after charging one electrode relative to the other, one electrode will have released all cations, and then the process stops (voltages get very high). Therefore, intercalation materials must be pre-charged in a suitable way such that

the full capacity of the pair of electrodes can be used [18].

For *asymmetric* electrodes, with a cathode and an anode fabricated from different materials, anodes have been constructed from:

1. Ag/AgCl
2. Activated carbon (AC)
3. Bismuth, Bi/BiOCl
4. MnO$_2$

The most common choices for anode materials in cells with an intercalation cathode is Ag/AgCl and activated carbon electrodes. The Ag/AgCl electrode only operates with the Cl$^-$ ions and therefore, it lacks the versatility provided by the activated carbon or cells with the same electrodes. The use of activated carbon provides a predictable capacitive behavior to the cell. However, having a smaller SAC per gram than the intercalation materials would mean a larger amount of carbon to be employed to match the intercalation electrode. Recently, bismuth (Bi) has been reported to be a potential anode material which can be coupled with an intercalation electrode [64]. In more detail, it has been demonstrated that Bi/BiOCl as an anode material can store ~80 mg of Cl$^-$ ions per gram of Bi (for a 600 mM NaCl solution) which is significantly higher than reported for conventional CDI systems. Slow reduction kinetics and loss of capacity (60% retention after 200 cycles at 20 A/m^2) were identified as the shortcomings of Bi/BiOCl as an anode. The electrical potential for the reduction step was reported to be in between 1.2 and 1.5 V vs. Ag/AgCl, which is more negative than values usually reported in literature. A CDI cell with MnO$_2$ electrode has also been proposed as an alternative to CDI cells with carbon electrodes [74]. The use of such a cell with a modified activated carbon cathode gave an enhanced stability in terms of SAC retention, in addition to increasing the value of SAC (14 mg/g) and reducing the parasitic reactions associated with carbon anodes. The redox reaction typically observed in MnO$_2$ is similar to that seen for PBAs [40]. It is worth noting that more effort has been put into the development of cathode materials in comparison to that for the anode. However, if the symmetrical electrode cell architecture would be further optimized, there may not be a need for a separate anode material.

3.2. Operation parameters

The desalination of brackish water depends on several operation parameters. Most important among them are the current density (i.e. the current applied per unit electrode area, A/m^2) and the salt concentration. These two factors have consequences for the SAC of the desalination cell. The studies reported in this review use different values for these parameters resulting in different capacities for salt adsorption. A glimpse of such differences in operating conditions and their effect on cell performance is illustrated in Fig. 3 which provides an overview of the SACs reported in different studies and the corresponding operational conditions such as the applied current/potential and the salt concentration. In addition, it also indicates the electrode (*E*) materials (anode (*A*) and cathode (*C*)) used in the desalination cell. A common characteristic observed during desalination experiments is the dependence of the total SAC on the salt concentration, the current density (for a constant current operation as shown in orange) and the voltage (for a constant voltage operation as shown in blue). A usual trend observed for constant-current operations is that an increase in the current density, while keeping the cut-off voltage and concentration the same, will increase the rate of salt adsorption but decreases the total salt adsorption in a cycle. This is due to an increase in the Ohmic drop (*IR*) in the cell which raises the cell voltage closer to the cut-off value leading to a reduction in the cycle time. For a given value of the applied current/voltage, an increase in the salt concentration increases the salt adsorption capacity only up to a certain extent [32]. An increase in salt concentration should decrease the energy consumed by the cell for desalination due to reduction in ionic resistance.
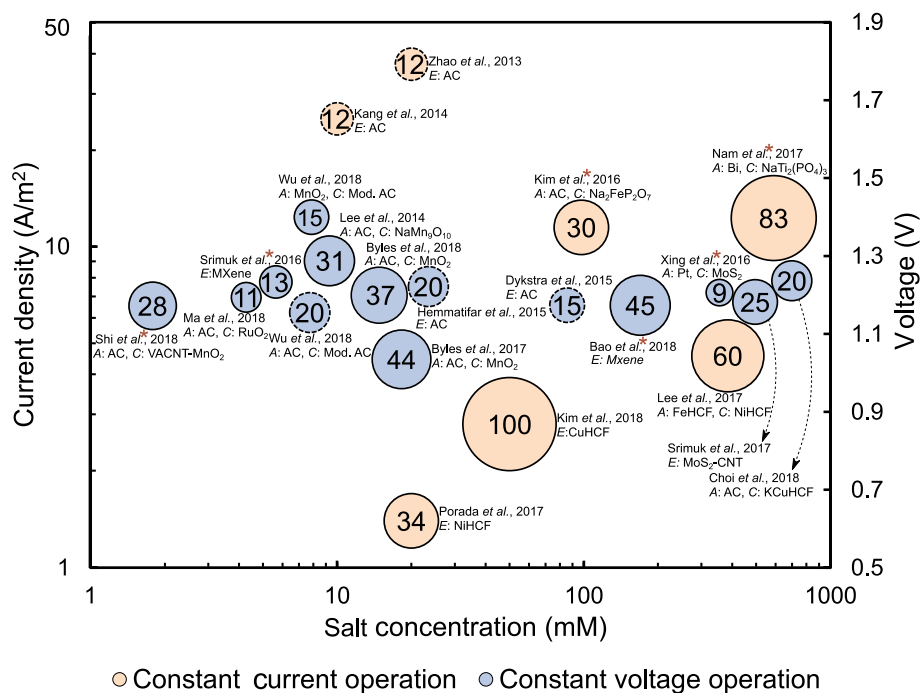
Fig. 3. An overview of salt adsorption capacities (SAC) in mg/g (total electrode mass, unless marked by a *), reported in literature for constant current (blue - left y-axis) and constant voltage (orange - right y-axis) operation as a function of applied current density (A/m²), salt concentration (mM) and applied voltage (V). The area of the circles is proportional to SAC (value given within the circles). The data labels give the information about the publication reporting the value along with the electrode (E) materials, indicated as cathode (C) and anode (A), used for the cell. A dashed circumference of the data-point circle represents SAC for carbon electrodes, added for comparison purposes.

It is interesting to realize that CDI with intercalation materials, in terms of the high SAC values observed, has been successfully applied to systems with salinities as low as 5 mM [58] and as high as 600 mM [64]. The largest value of 86 mg/(g-active material) for SAC was reported for a CDI cell with a Bi anode and a $NaTi_2(PO_4)_3$ cathode for a 600 mM salt solution, operating at a constant current of 10 A/m². Similarly, for a constant-voltage operation, the highest SAC of ~30 mg/(g-both electrodes) was reported for a salt solution with concentration from 10 to 100 mM operated at 1.2 V [32]. The charge capacity (usually reported in mAh/g) of the electrodes must also be considered along with the SAC values as it provides an idea about the system's ability to use the potential of the electrode for desalination. In addition to giving insight in the performance of the intercalation electrodes, Fig. 3 also provides an estimate of the range of values for SAC (and the operation parameters at which they were obtained) for carbon electrodes in CDI. It is difficult to compare the performance of intercalation and carbon electrodes, but some general features can be highlighted. The SAC values recorded for intercalation electrodes tend to be higher than those reported for carbon electrodes (values plotted in Fig. 3, with dashed data points, can be found in [20,23,85–87]). For instance, intercalation electrodes prepared from NiHCF, when immersed in a 20 mM salt solution, result in a SAC of 34 mg/g at an operating current of 1.4 A/m² [18]. On the other hand, carbon electrodes immersed in a 20 mM salt solution and operated at 37 A/m² achieved a SAC of 12 mg/g [20]. For constant voltage experiments, SAC values of 20 mg/g were reported for carbon electrodes for a salt concentration of 9 mM [23] and 20 mM [86]. These values were still smaller than those reported for intercalation electrodes operated under constant voltage for a similar salt concentration [32].

In addition to SAC, the average salt adsorption rate (ASAR) (reported in mg/g/s) is also an important parameter in CDI [7]. This parameter is influenced by the applied current or voltage. Consequently, ASAR in a constant current process increases with the current density [7,88]. Carbon electrodes can sustain high current densities and reach a high SAC at the same time [20,87]. However, unlike carbon electrodes, intercalation electrodes are not capable of maintaining a high SAC at high current densities as the charge capacity (in mAh/g) decreases with the charging rate [33]. It is indicative of the presence of limitations in one of the transport processes involved in desalination

with intercalation electrodes [35]. Therefore, for intercalation electrodes, at the moment an increase in the ASAR value comes at the expense of the SAC (reported in a Ragone plot in Fig. 7 of [33]). This is an interesting opportunity for the optimization of cell design and operation parameters to ensure both a high salt adsorption capacity and a high salt adsorption rate.

In addition to illustrating the performance numbers reported in literature, Fig. 3 also highlights the underlying difficulty in comparing different studies. This is due to different materials, experimental conditions, modes of operation (constant current vs. constant voltage) and reporting of results. The performance metrics for an objective assessment of the CDI performance and their comparison has been recently described in [89] highlighting certain general characteristics which may be helpful in comparing two desalination systems with different designs. This timeline attempts to provide clear information on the mass by which the SAC values are normalized. It usually varies from the mass of both electrodes [18,26] to the mass of active particles [64,65], which may be very different, particularly when (inactive) electrode supports are used. Therefore, to begin a meaningful comparison of desalination cell performances, parameters such as salt concentration, applied current/voltage, mass used for normalization of SAC, and cell architecture, must be explicitly mentioned.

4. Outlook

The discovery of redox activity in Prussian Blue (PB) in 1978 turned out to be a key moment in the development of intercalation electrodes. Since then, the study of the electrochemical properties of intercalation electrodes gradually expanded, with a systematic effort to understand and explain the redox-active behavior of intercalation electrodes. Remarkably, the electrochemical characteristics of the analogues of PB were studied soon after the electronic activity of pure PB was discovered. As a result, there is a considerable amount of literature which explains the characteristics of various PBAs. However, these materials were not immediately employed for water desalination. This occurred only after it was demonstrated that they were suitable for sodium ion batteries. In addition to PB(A), redox-activity has been discovered more recently in other materials, including MnO_2, $Na_2FeP_2O_7$, and MoS_2, which subsequently were successfully used in CDI. All of these electrode

materials show high rate capabilities and capacities and have potential for application in aqueous media.

A general rule for the optimization of intercalation materials and electrodes is that a high rate of salt removal must be achieved, while the salt adsorption capacity must at least be reasonable. To achieve this optimum, a systematic study is required of the dependence of cell performance on applied current/voltage and salt concentration. Furthermore, different studies have utilized different configurations of the desalination cell design. This includes the use of different cathode and anode materials (e.g., Ag/AgCl, carbon or another intercalation electrode), use of multiple membranes between the electrodes, and the position of the flow channel. A definitive optimization of geometric parameters, along with a standardized set of metrics for performance measurement of a desalination cell will be crucial to the development of intercalation electrodes in CDI. This will also make a performance comparison with existing technologies more convenient. Accepting the major differences between intercalation and carbon electrodes, nevertheless inspiration for optimization of desalination with intercalation electrodes can still be derived from the extensively developed CDI literature on carbon electrodes.

The chemistry of intercalation electrode materials offers avenues for the further development of the electrode structure, for example in terms of their stability, loading capacity, and selectivity. Depending on the type of electrode material and the electrode properties of interest, pre-synthetic and/or post-synthetic strategies may be followed. Following literature on energy storage applications [10] and medical diagnosis and treatment [90], NiHCF and other PBAs used in CDI studies are usually prepared via co-precipitation and, to a lesser extent, thin film electrodeposition, where water is the solvent of choice. In aqueous approaches it is a challenge to control the size of the particle agglomerates, which is relevant because of its role in controlling the accessibility both of ions and electronic charge to the active site. It is anticipated that the CDI field will benefit from recent developments in controlling PB and PBA nanostructure formation and morphology [90].

So far in CDI applications, NMO has been synthesized under high-temperature conditions using a solid-state reaction [32], before mixing with carbon black and a binder to obtain sheet-type electrodes. Given the versatility of the NMO system and its derivatives [91], there is a considerable research activity in this area, and chemical recipes from the field of energy storage will also become available to the field of CDI.

The MXene sheets [92] that have been introduced in CDI [58,73] are made by wet etching from their layered precursors. Delamination of MXene via intercalation approaches using polar organic molecules or large organic base molecules have been reported, and bottom-up methods such as chemical vapor deposition (CVD) are within reach [92]. In the case of another 2D material, MoS_2 nanosheets were prepared via an exfoliation technique, before depositing them onto gold-covered, flexible electrodes [61].

While the above-mentioned electrode materials have (some) size-based selectivity, the preparation of composite materials and post-synthetic treatments have the potential to further tune the intercalation of certain ions. In this regard, CDI can benefit from surface modification strategies already applied to carbon electrodes [6,93], but also to the field of water purification membranes [94]. Interestingly, polymer coatings can not only be tailored to control ion selectivity [95], but also to reduce fouling [96]. Another interesting development is the use of graphene-based materials in CDI technology [97]. Given its unique physicochemical properties, including the exceptionally high surface area, electron mobility, and mechanical strength, graphene is expected to be further integrated with intercalation materials, both in terms of composites as well as surface modification.

For further development of CDI technology, it is anticipated that inspiration will be taken from the already highly developed energy storage field [10]. Composites containing intercalation materials are interesting to achieve enhanced conductivity and higher structural stability. Post-synthetic surface modifications to obtain materials such

as polymer and graphene layers with a thickness in the nanometer scale, are attractive to deposit thin membrane layers on intercalation materials. The number of materials that are available as electrode building blocks, i.e. intercalation materials, polymers and fillers, is large and continues to increase. The main challenge is to develop chemical schemes which combine aspects related to the high structural stability and ion selectivity, and thus enabling the fabrication of electrodes with a long-term cycling stability that can also be applied in the selective removal and recovery of specific ions.

In addition, theoretical modeling of a complete CDI cell based on intercalation electrodes, has only recently been initiated. The modeling of ion transport and adsorption leads to a better understanding of the underlying physical processes and provides a tool for quantitative optimization of the parameters involved. Physics-based modeling uses a sufficiently detailed picture of the basic microscopic phenomena in ion transport and adsorption and implements this information in a large-scale model of a CDI cell. Therefore, it can analyze full CDI cycles and provide predictions for desalination, energy use and pH fluctuations. Such models exist for CDI with carbon-based electrodes, but their development is still in its early stages for CDI with intercalation materials [35,36,98].

For CDI with intercalation materials, on a microscopic level, questions to be addressed relate to the rate-limiting steps in ion adsorption in the electrodes. This limitation can have many causes, such as: the ion transport process within macropores that connect to the active particles [35]; the ion intercalation at the active particle-electrolyte interface [99]; the ion diffusion within the active particles [100]; or perhaps, dependent on electrode design, the electronic transport to and through the active particles [101]. A related question is the choice of the most suitable theoretical framework: is a model based on approaches similar to those used for batteries more suitable [36,59], or are the models based on dilute solutions and classical carbon electrodes [21] a better starting point? Other elements in a theoretical model that must be considered are the fluid flow pattern in the flow channels, and ion transport in the IEMs. An empirical description for the IEMs can be provided with a fixed value for ion selectivity, or a more detailed model can be used that describes diffusion and electromigration of all ions in the membrane. For the flow channels, a single stirred tank approach may suffice, but more detailed models can be used which include concentration gradients across the channel, as well as fluid flow patterns. Existing models [35,36,98] are based on one and two-dimensional numerical frameworks. Although this level of description is relevant, such models are also complicated to implement if experience in numerical programming is not available. Therefore zero-order models are also relevant to develop. Such models include the basic phenomena of ion transport and adsorption, but only use stirred tank approaches and describe transport limitations by an equivalent of Ohm's law or a film layer. Therefore, the model mainly consists of algebraic equations supplemented with macroscopic balances (described by ordinary differential equations) which describe the accumulation of ions in electrode and spacer. Such a model is easier to develop and implement than the higher-order models. Another future model extension is to consider separation of salt mixtures with intercalation materials [18,63].

The models discussed so far can be classified as mean-field or engineering models. Advanced theoretical tools and numerical methods are of relevance both on a small and larger scale. On the molecular scale, Molecular Dynamics (MD) simulations give insight in the intercalation process by looking at ion distributions and the capacity to store charge and ions. On the cell level, computational fluid dynamics (CFD) can help in describing fluid flow patterns inside the macropores of the electrode and in the flow channels. Knowledge obtained by these advanced tools must be translated (e.g., via empirical equations) for meaningful application in mean field/engineering models.

To conclude, studies on CDI with intercalation materials have been appearing in literature faster than ever. Experimental data for various operation parameters with different types of electrode materials are

now readily available. Therefore, the validation of theoretical models with the experimental data will be significantly facilitated. This may lead to faster system optimization and a better design of electrodes and cell, resulting in reduced energy consumption while improving desalination performance. For intercalation materials in CDI, endeavors in this direction will become important over the coming years.

Acknowledgement

References

[1] P.M. Biesheuvel, et al., Capacitive deionization–defining a class of desalination technologies, (2017) (arXiv1709.05925).

[2] Z.-H. Huang, Z. Yang, F. Kang, M. Inagaki, Carbon electrodes for capacitive deionization, J. Mater. Chem. A 5 (2) (2017) 470–496.

[3] M. Li, H.G. Park, Pseudocapacitive coating for effective capacitive deionization, ACS Appl. Mater. Interfaces 10 (3) (2018) 2442–2450.

[4] C. Kim, P. Srimuk, J. Lee, S. Fleischmann, M. Aslan, V. Presser, Influence of pore structure and cell voltage of activated carbon cloth as a versatile electrode material for capacitive deionization, Carbon 122 (2017) 329–335.

[5] S. Porada, R. Zhao, A. Van Der Wal, V. Presser, P.M. Biesheuvel, Review on the science and technology of water desalination by capacitive deionization, Prog. Mater. Sci. 58 (8) (2013) 1388–1442.

[6] Y. Liu, C. Nie, X. Liu, X. Xu, Z. Sun, L. Pan, Review on carbon-based composite materials for capacitive deionization, RSC Adv. 5 (20) (2015) 15205–15225.

[7] M.E. Suss, S. Porada, X. Sun, P.M. Biesheuvel, J. Yoon, V. Presser, Water desalination via capacitive deionization: what is it and what can we expect from it? Energy Environ. Sci. 8 (8) (2015) 2296–2319.

[8] A. Paolella, et al., A review on hexacyanoferrate-based materials for energy storage and smart windows: challenges and perspectives, J. Mater. Chem. A 5 (36) (2017) 18919–18932.

[9] F. Ma, Q. Li, T. Wang, H. Zhang, G. Wu, Energy storage materials derived from Prussian blue analogues, Sci. Bull. 62 (5) (2017) 358–368.

[10] M.E. Suss, V. Presser, Water desalination with energy storage electrode materials, Joule 2 (1) (2018) 25–35.

[11] X. Su, T.A. Hatton, Redox-electrodes for selective electrochemical separations, Adv. Colloid Interf. Sci. 244 (2017) 6–20.

[12] S.Y. Pan, S.W. Snyder, Y.J. Lin, P.C. Chiang, Electrokinetic desalination of brackish water and associated challenges in the water and energy nexus, Environ. Sci. Water Res. Technol. 4 (5) (2018) 613–638.

[13] J.F. Whitacre, A. Tevar, S. Sharma, Na₄Mn₉O₁₈ as a positive electrode material for an aqueous electrolyte sodium-ion energy storage device, Electrochem. Commun. 12 (3) (2010) 463–466.

[14] H. Kim, et al., Na₂FeP₂O₇ as a promising iron-based pyrophosphate cathode for sodium rechargeable batteries: a combined experimental and theoretical study, Adv. Funct. Mater. 23 (9) (2012) 1147–1155.

[15] Y. Lu, L. Wang, J. Cheng, J.B. Goodenough, Prussian blue: a new framework of electrode materials for sodium batteries, Chem. Commun. 48 (52) (2012) 6544–6546.

[16] J.W. Blair, G.W. Murphy, Electrochemical demineralization of water with porous electrodes of large surface area, Saline Water Conversion, Ch. 20 1960, pp. 206–223.

[17] G.W. Murphy, D.D. Caudle, Mathematical theory of electrochemical demineralization in flowing systems, Electrochim. Acta 12 (12) (1967) 1655–1664.

[18] S. Porada, A. Shrivastava, P. Bukowska, P.M. Biesheuvel, K.C. Smith, Nickel hexacyanoferrate electrodes for continuous cation intercalation desalination of brackish water, Electrochim. Acta 255 (2017) 369–378.

[19] P.M. Biesheuvel, R. Zhao, S. Porada, A. van der Wal, Theory of membrane capacitive deionization including the effect of the electrode pore space, J. Colloid Interface Sci. 360 (1) (2011) 239–248.

[20] R. Zhao, O. Satpradit, H.H.M. Rijnaarts, P.M. Biesheuvel, A. van der Wal, Optimization of salt adsorption rate in membrane capacitive deionization, Water Res. 47 (5) (2013) 1941–1952.

[21] P.M. Biesheuvel, A. van der Wal, Membrane capacitive deionization, J. Membr. Sci. 346 (2) (2010) 256–262.

[22] Y.J. Kim, J.H. Choi, Improvement of desalination efficiency in capacitive deionization using a carbon electrode coated with an ion-exchange polymer, Water Res. 44 (3) (2010) 990–996.

[23] T. Wu, et al., Surface-treated carbon electrodes with modified potential of zero charge for capacitive deionization, Water Res. 93 (2016) 30–37.

[24] T. Ikeshoji, Separation of alkali metal ions by intercalation into a Prussian blue electrode, J. Electrochem. Soc. 133 (10) (1986) 2108–2109.

[25] R. Zhao, M. Van Soestbergen, H.H.M. Rijnaarts, A. Van der Wal, M.Z. Bazant, P.M. Biesheuvel, Time-dependent ion selectivity in capacitive charging of porous electrodes, J. Colloid Interface Sci. 384 (1) (2012) 38–44.

[26] T. Kim, C.A. Gorski, B.E. Logan, Low energy desalination using battery electrode deionization, Environ. Sci. Technol. Lett. 4 (10) (2017) 444–449.

[27] J.E. Dykstra, J. Dijkstra, A. Van der Wal, H.V.M. Hamelers, S. Porada, On-line method to study dynamics of ion adsorption from mixtures of salts in capacitive deionization, Desalination 390 (2016) 47–52.

[28] J. Choi, H. Lee, S. Hong, Capacitive deionization (CDI) integrated with monovalent cation selective membrane for producing divalent cation-rich solution, Desalination 400 (2016) 38–46.

[29] P.G. Campbell, et al., Selective ion removal from water using flow-through electrode capacitive deionization (fteCDI), Meeting Abstracts, J. Electrochem. Soc. 20 (2018) 1284.

[30] K. Zuo, et al., Novel composite electrodes for selective removal of sulfate by the capacitive deionization process, Environ. Sci. Technol. 52 (16) (2018) 9486–9494.

[31] M.E. Suss, Size-based ion selectivity of micropore electric double layers in capacitive deionization electrodes, J. Electrochem. Soc. 164 (9) (2017) E270–E275.

[32] J. Lee, S. Kim, C. Kim, J. Yoon, Hybrid capacitive deionization to enhance the desalination performance of capacitive techniques, Energy Environ. Sci. 7 (11) (2014) 3683–3689.

[33] S. Kim, J. Lee, C. Kim, J. Yoon, Na₂FeP₂O₇as a novel material for hybrid capacitive deionization, Electrochim. Acta 203 (2016) 265–271.

[34] J. Lee, S. Kim, J. Yoon, Rocking chair desalination battery based on Prussian blue electrodes, ACS Omega 2 (4) (2017) 1653–1659.

[35] K. Singh, H.J.M. Bouwmeester, L. de Smet, M.Z. Bazant, P.M. Biesheuvel, Theory of water desalination with intercalation materials, Phys. Rev. Appl. 9 (6) (2018) 64036–64045.

[36] K.C. Smith, R. Dmello, Na-ion desalination (NID) enabled by Na-blocking membranes and symmetric Na-intercalation: porous-electrode modeling, J. Electrochem. Soc. 163 (3) (2016) A530–A539.

[37] V.D. Neff, Electrochemical oxidation and reduction of thin films of Prussian blue, J. Electrochem. Soc. 125 (6) (1978) 886–887.

[38] M.R. Lukatskaya, et al., Cation intercalation and high volumetric capacitance of two-dimensional titanium carbide, Science 341 (6153) (2013) 1502–1505.

[39] P. Marzak, et al., Electrodeposited Na₂Ni[Fe(CN)₆] thin-film cathodes exposed to simulated aqueous Na-ion battery conditions, J. Phys. Chem. C 122 (16) (2018) 8760–8768.

[40] A.A. Karyakin, Prussian Blue and Its Analogues: Electrochemistry and Analytical Applications, 10 (2001), pp. 813–819.

[41] L.F. Schneemeyer, S.E. Spengler, D.W. Murphy, Ion selectivity in nickel hexacyanoferrate films on electrode surfaces, Inorg. Chem. 24 (19) (1985) 3044–3046.

[42] C.D. Wessells, S.V. Peddada, M.T. McDowell, R.A. Huggins, Y. Cui, The effect of insertion species on nanostructured open framework hexacyanoferrate battery electrodes, J. Electrochem. Soc. 159 (2) (2012) A98–A103.

[43] M. Naguib, V.N. Mochalin, M.W. Barsoum, Y. Gogotsi, 25th anniversary article: MXenes: a new family of two-dimensional materials, Adv. Mater. 26 (7) (2014) 992–1005.

[44] A.B. Bocarsly, S. Sinha, Effects of surface structure on electrode charge transfer properties. Induction of ion selectivity at the chemically derivatized interface, J. Electroanal. Chem. 140 (1) (1982) 167–172.

[45] M.A. Lilga, R.J. Orth, J.P.H. Sukamto, S.M. Haight, D.T. Schwartz, Metal ion separations using electrically switched ion exchange, Sep. Purif. Technol. 11 (3) (1997) 147–158.

[46] S.D. Rassat, J.H. Sukamto, R.J. Orth, M.A. Lilga, R.T. Hallen, Development of an electrically switched ion exchange process for selective ion separations, Sep. Purif. Technol. 15 (3) (1999) 207–222.

[47] J. Yang, L. Zou, H. Song, Z. Hao, Development of novel MnO2/nanoporous carbon composite electrodes in capacitive deionization technology, Desalination 276 (1–3) (2011) 199–206.

[48] C.Z. Yuan, B. Gao, L.H. Su, X.G. Zhang, Interface synthesis of mesoporous MnO2and its electrochemical capacitive behaviors, J. Colloid Interface Sci. 322 (2) (2008) 545–550.

[49] S. Il Park, I. Gocheva, S. Okada, J. Yamaki, Electrochemical properties of NaTi₂(PO₄)₃ anode for rechargeable aqueous sodium-ion batteries, J. Electrochem. Soc. 158 (10) (2011) A1067–A1070.

[50] C.D. Wessells, S.V. Peddada, R.A. Huggins, Y. Cui, Nickel hexacyanoferrate nanoparticle electrodes for aqueous sodium and potassium ion batteries, Nano Lett. 11 (12) (2011) 5421–5425.

[51] M. Pasta, C.D. Wessells, Y. Cui, F. La Mantia, A desalination battery, Nano Lett. 12 (2) (2012) 839–843.

[52] B. Sun, et al., Separation of low concentration of cesium ion from wastewater by electrochemically switched ion exchange method: experimental adsorption kinetics analysis, J. Hazard. Mater. 233–234 (2012) 177–183.

[53] R. Chen, et al., Selective removal of cesium ions from wastewater using copper hexacyanoferrate nanofilms in an electrochemical system, Electrochim. Acta 87 (2013) 119–125.

[54] C. Weidlich, K.M. Mangold, K. Jüttner, Continuous ion exchange process based on polypyrrole as an electrochemically switchable ion exchanger, Electrochim. Acta 50 (25) (2005) 5247–5254.

[55] R. Chen, H. Tanaka, T. Kawamoto, J. Wang, Y. Zhang, Battery-type column for

caesium ions separation using electroactive film of copper hexacyanoferrate nanoparticles, Sep. Purif. Technol. 173 (2017) 44–48.

[56] B. Chen, et al., Enhanced capacitive desalination of MnO_2 by forming composite with multi-walled carbon nanotubes, RSC Adv. 6 (8) (2016) 6730–6736.

[57] A.L. Lipson, et al., Nickel hexacyanoferrate, a versatile intercalation host for divalent ions from nonaqueous electrolytes, J. Power Sources 325 (2016) 646–652.

[58] P. Srimuk, et al., MXene as a novel intercalation-type pseudocapacitive cathode and anode for capacitive deionization, J. Mater. Chem. A 4 (47) (2016) 18265–18271.

[59] K.C. Smith, Theoretical evaluation of electrochemical cell architectures using cation intercalation electrodes for desalination, Electrochim. Acta 230 (2017) 333–341.

[60] F. Xing, T. Li, J. Li, H. Zhu, N. Wang, X. Cao, Chemically exfoliated MoS_2 for capacitive deionization of saline water, Nano Energy 31 (2017) 590–595.

[61] M. Acerce, D. Voiry, M. Chhowalla, Metallic 1T phase MoS_2 nanosheets as supercapacitor electrode materials, Nat. Nanotechnol. 10 (4) (2015) 313–318.

[62] S. Porada, P. Bukowska, A. Shrivastava, P.M. Biesheuvel, K.C. Smith, Nickel hexacyanoferrate electrodes for cation intercalation desalination, arXiv1612.08293, (2016).

[63] C. Erinmwingbovo, M.S. Palagonia, D. Brogioli, F. La Mantia, Intercalation into a Prussian blue derivative from solutions containing two species of cations, ChemPhysChem 18 (8) (2017) 917–925.

[64] D.-H. Nam, K.-S. Choi, Bismuth as a new chloride-storage electrode enabling the construction of a practical high capacity desalination battery, J. Am. Chem. Soc. 139 (32) (2017) 11055–11063.

[65] F. Chen, Y. Huang, L. Guo, M. Ding, H.Y. Yang, A dual-ion electrochemistry deionization system based on $AgCl-Na_{0.44}MnO_2$ electrodes, Nanoscale 9 (28) (2017) 10101–10108.

[66] P. Srimuk, et al., Faradaic deionization of brackish and sea water via pseudocapacitive cation and anion intercalation into few-layered molybdenum disulfide, J. Mater. Chem. A 5 (30) (2017) 15640–15649.

[67] S. Kim, H. Yoon, D. Shin, J. Lee, J. Yoon, Electrochemical selective ion separation in capacitive deionization with sodium manganese oxide, J. Colloid Interface Sci. 506 (2017) 644–648.

[68] L. Guo, et al., A Prussian blue anode for high performance electrochemical deionization promoted by the faradaic mechanism, Nanoscale 9 (35) (2017) 13305–13312.

[69] H. Yoon, J. Lee, S. Kim, J. Yoon, Electrochemical sodium ion impurity removal system for producing high purity KCl, Hydrometallurgy 175 (2018) 354–358.

[70] B.W. Byles, D.A. Cullen, K.L. More, E. Pomerantseva, Tunnel structured manganese oxide nanowires as redox active electrodes for hybrid capacitive deionization, Nano Energy 44 (2018) 476–488.

[71] J. Lee, et al., Pseudocapacitive desalination of brackish water and seawater with vanadium-pentoxide-decorated multiwalled carbon nanotubes, ChemSusChem 10 (18) (2017) 3611–3623.

[72] P. Srimuk, J. Lee, A. Tolosa, C. Kim, M. Aslan, V. Presser, Titanium disulfide: a promising low-dimensional electrode material for sodium ion intercalation for seawater desalination, Chem. Mater. 29 (23) (2017) 9964–9973.

[73] W. Bao, et al., Porous cryo-dried MXene for efficient capacitive deionization, Aust. Dent. J. 2 (4) (2018) 778–787.

[74] T. Wu, et al., Highly stable hybrid capacitive deionization with a MnO_2 anode and a positively charged cathode, Environ. Sci. Technol. Lett. 5 (2) (2018) 98–102.

[75] S. Liu, K.C. Smith, Quantifying the trade-offs between energy consumption and salt removal rate in membrane-free cation intercalation desalination, Electrochim. Acta 271 (2018) 652–665.

[76] P. Srimuk, J. Lee, S. Fleischmann, M. Aslan, C. Kim, V. Presser, Potential-dependent, switchable ion selectivity in aqueous media using titanium disulfide, ChemSusChem 11 (13) (2018) 2091–2100.

[77] S. Choi, B. Chang, S. Kim, J. Lee, J. Yoon, J.W. Choi, Battery electrode materials with omnivalent cation storage for fast and charge-efficient ion removal of asymmetric capacitive deionization, Adv. Funct. Mater. 28 (35) (2018) 1802665.

[78] X. Ma, Y.-A. Chen, K. Zhou, P.-C. Wu, C.-H. Hou, Enhanced desalination performance via mixed capacitive-Faradaic ion storage using RuO_2-activated carbon composite electrodes, Electrochim. Acta 295 (2019) 769–777.

[79] B.W. Byles, B. Hayes-Oberst, E. Pomerantseva, Ion removal performance,

[80] structural/compositional dynamics, and electrochemical stability of layered manganese oxide electrodes in hybrid capacitive deionization, ACS Appl. Mater. Interfaces 10 (38) (2018) 32313–32322.

[80] T. Kim, C.A. Gorski, B.E. Logan, Ammonium removal from domestic wastewater using selective battery electrodes, Environ. Sci. Technol. Lett. 5 (9) (2018) 578–583.

[81] W. Shi, et al., High-performance capacitive deionization via manganese oxide-coated, vertically aligned carbon nanotubes, Environ. Sci. Technol. Lett. 5 (11) (2018) 692–700.

[82] W. Zhao, L. Guo, M. Ding, Y. Huang, H.Y. Yang, Ultrahigh desalination capacity dual-ion electrochemical deionization device based on $Na_3V_2(PO_4)_3$@C-AgCl electrodes, ACS Appl. Mater. Interfaces 10 (47) (2018) 40540–40548.

[83] L. Agartan, B. Hayes-Oberst, B.W. Byles, B. Akuzum, E. Pomerantseva, E.C. Kumbur, Influence of operating conditions and cathode parameters on desalination performance of hybrid CDI systems, Desalination 452 (2019) 1–8.

[84] P. Srimuk, J. Halim, J. Lee, Q. Tao, J. Rosen, V. Presser, Two-dimensional molybdenum carbide (MXene) with divacancy ordering for brackish and seawater desalination via cation and anion intercalation, ACS Sustain. Chem. Eng. 6 (3) (2018) 3739–3747.

[85] J.E. Dykstra, R. Zhao, P.M. Biesheuvel, A. Van der Wal, Resistance identification and rational process design in capacitive deionization, Water Res. 88 (2016) 358–370.

[86] A. Hemmatifar, M. Stadermann, J.G. Santiago, Two-dimensional porous electrode model for capacitive deionization, J. Phys. Chem. C 119 (44) (2015) 24681–24694.

[87] J. Kang, T. Kim, K. Jo, J. Yoon, Comparison of salt adsorption capacity and energy consumption between constant current and constant voltage operation in capacitive deionization, Desalination 352 (2014) 52–57.

[88] J. Lee, et al., Confined redox reactions of iodide in carbon nanopores for fast and energy-efficient desalination of brackish water and seawater, ChemSusChem 11 (2018) 3460–3472.

[89] S.A. Hawks, et al., Performance metrics for the objective assessment of capacitive deionization systems, Water Res. (2018) (in press).

[90] M. Gautam, K. Poudel, C.S. Yong, J.O. Kim, Prussian blue nanoparticles: synthesis, surface modification, and application in cancer treatment, Int. J. Pharm. 549 (1–2) (2018) 712–749.

[91] M.H. Han, E. Gonzalo, G. Singh, T. Rojo, A comprehensive review of sodium layered oxides: powerful cathodes for Na-ion batteries, Energy Environ. Sci. 8 (1) (2015) 81–102.

[92] B. Anasori, M.R. Lukatskaya, Y. Gogotsi, 2D metal carbides and nitrides (MXenes) for energy storage, Nat. Rev. Mater. 2 (2) (2017) 16098.

[93] M.S. Gaikwad, C. Balomajumder, Polymer coated capacitive deionization electrode for desalination: a mini review, Electrochem. Energy Technol. 2 (1) (2016) 1–5.

[94] D.J. Miller, D.R. Dreyer, C.W. Bielawski, D.R. Paul, B.D. Freeman, Surface modification of water purification membranes, Angew. Chem. Int. Ed. 56 (17) (2017) 4662–4711.

[95] C. Cheng, A. Yaroshchuk, M.L. Bruening, Fundamentals of selective ion transport through multilayer polyelectrolyte membranes, Langmuir 29 (6) (2013) 1885–1892.

[96] J.B. Schlenoff, Zwitteration: coating surfaces with zwitterionic functionality to reduce nonspecific adsorption, Langmuir 30 (32) (2014) 9625–9636.

[97] L. Li, G. Zhou, Z. Weng, X.-Y. Shan, F. Li, H.-M. Cheng, Monolithic Fe_2O_3/graphene hybrid for highly efficient lithium storage and arsenic removal, Carbon 67 (2014) 500–507.

[98] K. West, T. Jacobsen, S. Atlung, Modeling of porous insertion electrodes with liquid electrolyte, J. Electrochem. Soc. 129 (7) (1982) 1480–1485.

[99] P. Bai, M.Z. Bazant, Charge transfer kinetics at the solid-solid interface in porous electrodes, Nat. Commun. 5 (2014) 3585.

[100] W. Weppner, Determination of the kinetic parameters of mixed-conducting electrodes and application to the system Li_3Sb, J. Electrochem. Soc. 124 (10) (1977) 1569–1578.

[101] A. Shrivastava, K.C. Smith, Electron conduction in nanoparticle agglomerates limits apparent Na^+ diffusion in Prussian blue analogue porous electrodes, J. Electrochem. Soc. 165 (9) (2018) A1777–A1787.